



**HAL**  
open science

## Calathus: A sample-return mission to Ceres

Oriane Gassot, Paolo Panicucci, Giacomo Acciarini, Helena Bates, Manel Caballero, Pamela Cambianica, Maciej Dziewiecki, Zelia Dionnet, Florine Enengl, Selina-Barbara Gerig, et al.

► **To cite this version:**

Oriane Gassot, Paolo Panicucci, Giacomo Acciarini, Helena Bates, Manel Caballero, et al..  
Calathus: A sample-return mission to Ceres. Acta Astronautica, 2021, 181, pp.112-129.  
10.1016/j.actaastro.2020.12.050 . insu-03559381

**HAL Id: insu-03559381**

**<https://insu.hal.science/insu-03559381>**

Submitted on 13 Feb 2023

**HAL** is a multi-disciplinary open access archive for the deposit and dissemination of scientific research documents, whether they are published or not. The documents may come from teaching and research institutions in France or abroad, or from public or private research centers.

L'archive ouverte pluridisciplinaire **HAL**, est destinée au dépôt et à la diffusion de documents scientifiques de niveau recherche, publiés ou non, émanant des établissements d'enseignement et de recherche français ou étrangers, des laboratoires publics ou privés.



Distributed under a Creative Commons Attribution - NonCommercial 4.0 International License

# Calathus: A Sample-Return Mission to Ceres

Oriane Gassot<sup>a</sup>, Paolo Panicucci<sup>b,c,d</sup>, Giacomo Acciarini<sup>e</sup>, Helena Bates<sup>f,g</sup>, Manel Caballero<sup>h</sup>, Pamela Cambianica<sup>i</sup>, Maciej Dziewiecki<sup>j</sup>, Zelia Dionnet<sup>k</sup>, Florine Enengl<sup>l</sup>, Selina-Barbara Gerig<sup>m</sup>, Felix Hessinger<sup>n</sup>, Lucy Kissick<sup>o</sup>, Moritz Novak<sup>o</sup>, Carmine Pellegrino<sup>p</sup>, Angèle Pontoni<sup>q</sup>, Tânia M. Ribeiro<sup>r</sup>, Clemens Riegler<sup>s</sup>, Nini Berge<sup>t</sup>, Nikolaus Huber<sup>u</sup>, Richard Hynek<sup>v</sup>, Bartosz Kedziora<sup>w</sup>, Adam Kiss<sup>x</sup>, Maurice Martin<sup>y</sup>, Javier Navarro Montilla<sup>z</sup>

<sup>a</sup>Univ. Grenoble Alpes, CNRS, IPAG, 38000 Grenoble, France

<sup>b</sup>CNES, 18 Avenue Edouard Belin, 31400, Toulouse, France

<sup>c</sup>ISAE-SUPAERO, 10 Avenue Edouard Belin, 31400, Toulouse, France

<sup>d</sup>Airbus Defence & Space, 31 Rue des Cosmonautes, 31400 Toulouse, France

<sup>e</sup>University of Strathclyde

<sup>f</sup>Natural History Museum, London

<sup>g</sup>University of Oxford

<sup>h</sup>Universitat Politècnica de Catalunya

<sup>i</sup>INAF - Astronomical observatory of Padova, Vicolo dell'Osservatorio 5, 35122 Padova, Italy

<sup>j</sup>Wrocław University of Science and Technology

<sup>k</sup>Università degli studi di Napoli Parthenope

<sup>l</sup>KTH Royal Institute of Technology

<sup>m</sup>Physikalisches Institut, University of Bern, Sidlerstrasse 5, 3012 Bern, Switzerland

<sup>n</sup>Luleå University of Technology

<sup>o</sup>Vienna University of Technology

<sup>p</sup>Technical University of Munich, Institute for Nanoelectronics, 80333 Munich, Germany

<sup>q</sup>Swedish Institute of Space Physics, Kiruna, Sweden

<sup>r</sup>IFIMUP and Departamento de Física e Astronomia, Faculdade de Ciências da Universidade do Porto, Rua do Campo Alegre 687, 4169-007

Porto, Portugal

<sup>s</sup>JMU Würzburg

<sup>t</sup>Laboratoire de Physique et de Chimie de l'Environnement et de l'Espace, University of Orleans, CNRS

<sup>u</sup>Uppsala University

<sup>v</sup>University of West Bohemia

<sup>w</sup>Warsaw University of Technology

<sup>x</sup>Budapest University of Technology and Economics

<sup>y</sup>University of Stuttgart

<sup>z</sup>Institut National des Sciences Appliquées

## Abstract

Ceres, as revealed by NASA's Dawn spacecraft, is an ancient, crater-saturated body dominated by low-albedo clays. Yet, localised sites display a bright, carbonate mineralogy that may be as young as 2 Myr. The largest of these bright regions (faculae) are found in the 92 km Occator Crater, and would have formed by the eruption of alkaline brines from a subsurface reservoir of fluids. The internal structure and surface chemistry suggest that Ceres is an extant host for a number of the known prerequisites for terrestrial biota, and as such, represents an accessible insight into a potentially habitable 'ocean world'. In this paper, the case and the means for a return mission to Ceres are outlined, presenting the Calathus mission to return to Earth a sample of the Occator Crater faculae for high-precision laboratory analyses. Calathus consists of an orbiter and a lander with an ascent module: the orbiter is equipped with a high-resolution camera, a thermal imager, and a radar; the lander contains a sampling arm, a camera, and an on-board gas chromatograph mass spectrometer; and the ascent module contains vessels for four cerean samples, collectively amounting to a maximum 40 g. Upon return to Earth, the samples would be characterised via high-precision analyses to understand the salt and organic composition of the Occator faculae, and from there to assess both the habitability and the evolution of a relict ocean world from the dawn of the Solar System.

Preprint submitted to Elsevier

## 1. Introduction

The concept of a star's habitable zone — a region of astrobologically favourable warmth — has commensurately weakened with the growing understanding of the so-called *ocean worlds*. These are Solar System bodies that potentially contain sub-surface reservoirs of liquid water, whether global or local, definite or speculative [1]. Europa and Enceladus are the founding archetypes of this category [2, 3], but it is now understood that these encompass a much wider collection of Solar System bodies than first thought. From the Sun outward, Ceres, Ganymede, Callisto, Titan, Triton, Pluto, and Charon may host or have hosted subsurface liquid reservoirs [4, 5, 6], while additional outer worlds including Oberon, Titania, and Eris are a source of speculation [7]. Of these, geologically-recent activity is either observed or inferred for Europa, Enceladus, Triton, Ceres and Pluto, which moreover bear extrusions of their subsurface hydrosphere readily accessible upon their surface. Cryovolcanism has been widely conjectured in some form of Saturn's moon, Titan [8], and the Titan's thick atmosphere is considered as a strong argument in favor of recent activity [9], but the interpretation of Cassini data has been insufficient to demonstrate conclusively whether Titan is, or even has been, cryovolcanically active [9].

Ocean worlds are a focal point of interest in planetary science for presenting a convergence of the fundamental requirements for known life: a source of energy, a liquid solvent, and the resulting chemical gradients for mobilising biologically relevant elements including C, H, N, O, P, and S. All the active-to-dormant ocean worlds discussed above show evidence of the other known prerequisite for life, which is complex organics [10, 11, 12, 13, 14].

In this context, studying Ceres may solve remaining inquiries concerning the formation and evolution of planetary systems, and particularly the main belt. Based on the data from the Dawn mission, the surface of Ceres is consistent with aqueous alteration of CM chondrites [15], suggesting first that the largest object of the main belt could be a carbonaceous body, different from the non-carbonaceous body formed in the inner solar system [16], but also that that Ceres experienced global aqueous alteration. Dawn revealed Ceres as a volatile-rich body, with a partially differentiated interior, which experienced both cryovolcanism and geothermal activity in its recent history. Dawn revealed an ubiquitous presence of hydrated minerals, a distribution of ammoniated phyllosilicates [17, 18] linked to its formation, and a latitudinal variation of abundance of water ice [19] related to the evolution of its subsurface. The presence of subsurface volatiles can be inferred from many geomorphological features : the bright regions within the Occator crater are one of the most remarkable features observed by Dawn, and are the most direct evidence of recent geothermal activity on this body. Being an accessible potential ocean world, a sample return mission to Ceres is fundamental to investigate the astrobological significance of this body and its subsurface, being a potential favorable environment to prebiotic chemistry in a aqueous environment. [13].

In addition, sampling an accessible, possibly active, and under Class V protection (classification according to [20] and discussed in the section 4.6) ocean world would further our understanding of this growing class of ocean bodies and could be a forerunner in the development on future landing missions on different likely candidates for hosting extant life in the Solar System.

Here the Calathus mission concept [21, 22] is presented as it has been improved during the Post Alpbach Summer School Event held at the ESA Academy in Redu in 2018. Its aim is to return a sample from Ceres and characterise an ocean world with the full analytical capabilities in Earth-based laboratories. The mission concept is named after the basket which was carried from Ceres, the goddess of harvests, as symbol of abundance and fertility in the symbolic ancient Greek art.

### 1.1. Dawn's Ceres

Ceres, discovered by Giuseppe Piazzi in 1801 [18], holds a unique position among the small bodies of the Solar Systems. Ceres is the most massive body of the main asteroid belt, making up to the 30% of the entire belt's mass [23]. Its observation with Hubble Space Telescope revealed a complex scenario: more a proto-planet than an asteroid, with high-albedo features localized on the surface, and a low density body with stratified mantles and a silicate core [24, 25]. Because of these reasons, on 6 of March 2015, NASA's Dawn spacecraft [26] became the first human-made object to enter in orbit around Ceres, where it began investigations that lasted 3.5 years.

Shape and gravity measurements carried out by the Dawn spacecraft have been used to provide an estimation of Ceres' moment of inertia, which was in turn used to infer its internal structure and evolution, namely by determining its bulk density and rotation poles. The gravity data showed a celestial body with a mean crustal thickness between 27 and 43 km and a surface density between 1200 and 1600 kg/m<sup>3</sup> [27] which implies high water content [28]. Furthermore,

84 Dawn revealed a frigid ( $\sim 160$  K [29]), thoroughly cratered, extremely low albedo surface (0.09 [30]) with intermittent  
85 bright patches (named *faculae*) often within craters. This predominantly dark surface is comprised of hydroxylated  
86 material including ubiquitous Mg- and  $\text{NH}_4$ -bearing phyllosilicates and Mg-Ca carbonates [17, 18] alongside possible  
87 organic molecules [13] that bear similarity to carbonaceous chondrites, particularly the CI- and CM-types [31, 32, 33].  
88 This is consistent with a water-rich, partially-differentiated, carbonaceous and siliceous body.  
89 Craters are Ceres' most prevalent geomorphological feature. These are frequently fractured across their floors and,  
90 alongside kilometre-scale fractures not associated with impacts, may represent subsurface pressure rise associated  
91 with cryo-magmatic intrusion [34]. A 4 km-high dome named Ahuna Mons is a candidate cryo-volcano formed by  
92 the extrusion of such cryo-magma [35]. Unlike most of Ceres' ancient, cratered terrain, the flanks of Ahuna Mons  
93 are bright and relatively young — last resurfaced  $210 \pm 30$  Ma [35] — with a spectral signature corresponding to  
94 Mg-Ca- and Na-carbonates [36]. This is surprising in the context of Ceres' both minor solar insolation (at 2.8 AU)  
95 and diameter (at  $\sim 940$  km), neither of which are sufficient to explain such geologically recent activity.  
96 The most extraordinary indicator of a recently active subsurface, however, are the bright patches [4], or faculae. These  
97 features are defined as bright regions related to past or current outgassing [37], volcanism or resurfacing phenomena.  
98 These faculae are of an albedo five to ten times higher than the average cerean surface [38] and, in contrast to the  
99 phyllosilicate-dominated crust, are composed predominantly of anhydrous Na-carbonate ( $\text{Na}_2\text{CO}_3$ ), with minor hy-  
100 drated Na-carbonate, Al-phyllosilicates, and  $\text{NH}_4$ -chlorides [39, 40, 38].  
101 The largest of these exposures are within Occator Crater, in Figure 1. They are unique in both age — at their youngest  
102 estimate  $< 2$  Ma [41] — but also for their extent: together they cover over  $200 \text{ km}^2$  [39], making them the largest of  
103 their kind on Ceres, and one of the largest extraterrestrial carbonate deposits in the Solar System.  
104 Occator Crater is 92 km in diameter, centred at  $19.9^\circ \text{N}$ ,  $239.1^\circ \text{E}$ , and at maximum 4 km below the surrounding  
105 terrain [42]. While relatively flat-floored, the crater is pierced by a prominent central peak 2 km wide and 0.4 km  
106 high within a pit 9 km across and 1 km deep [42]. The crater's defining attributes are the faculae: these are Cerealia  
107 Facula, associated with the central pit/dome, and Vinalia Facula, which comprises several distinct, discontinuously  
108 spread faculae eastward of Cerealia towards the crater rim. The carbonates found in the faculae in Occator, in partic-  
109 ular natrite ( $\text{Na}_2\text{CO}_3$ ), are different from the Mg-Ca carbonate detected in the global Ceres spectrum [40]. Occator  
110 therefore represents the clearest insight into a process that was once widespread, perhaps planet-wide; a process that  
111 provides a window into both the ancient and the present cerean subsurface.  
112 With a draping morphology upon the floor of Occator, and an association with both doming and fracturing, the source  
113 of these bright carbonates is attributed to cryo-volcanic eruption as fountains of salt-rich water [39, 43]. Their salt-  
114 carbonate composition is consistent with the solid residue expected from alkaline brines formed by carbonaceous  
115 chondrite interaction with warm fluids: upon exiting the subsurface, the water component of such fluids instantly  
116 sublimates in the near-vacuum, leaving the solutes to rain back in the diffuse pattern observed by Dawn.  
117 The source of these fluids beneath Occator is likely a shallow subsurface reservoir: planetary evolution models sug-  
118 gest an ocean may have once existed at shallow depths [44], which may persevere today as localised brine reservoirs.  
119 The detection of salt compounds on Ceres' bright spots ( $\text{Na}_2\text{CO}_3$ ,  $\text{NH}_4\text{Cl}$  or  $\text{NH}_4\text{HCO}_3$ ) may be solid residues from  
120 the crystallization of brines that reached the surface from the interior ocean [39]. In addition, laboratory experiments  
121 support the outcome of this scenario [45], suggesting also that the detection  $\text{NH}_4\text{Cl}$  on Ceres' surface could imply that  
122 the ocean is rich in ammonium and/or chloride.

### 123 1.2. *The case for a return to Ceres*

124 The faculae of Occator Crater are the exposed interior of a water-rich body [43]. As water is one of the known  
125 prerequisites for biota as it is known on Earth, investigating the faculae gives an opportunity to investigate a potential  
126 habitable niche and may help our understanding of the variety of potential habitats in our Solar System. Ceres is the  
127 most readily accessible of the aforementioned *ocean worlds* to Earth, both as the closest but as one already thoroughly  
128 characterised by Dawn. A return to Ceres with the explicit intent to study Occator Crater is to stand upon the shoulders  
129 of Dawn to see further still into the workings of a potentially habitable body [4].

130 A second clear case for the return to Ceres looks not to Ceres' present but to life origins. Ceres' spectral signature does  
131 not match any known meteorite clan, which is unusual given both its large mass and the strong connection between cer-  
132 tain meteorites and similarly-sized planetesimals (e.g., the Howardite-Eucrite-Diogenite clan and Vesta [46]). Ceres  
133 is carbonaceous and most closely aligned to CI- and CM-type chondrites, which are strongly aqueously altered and

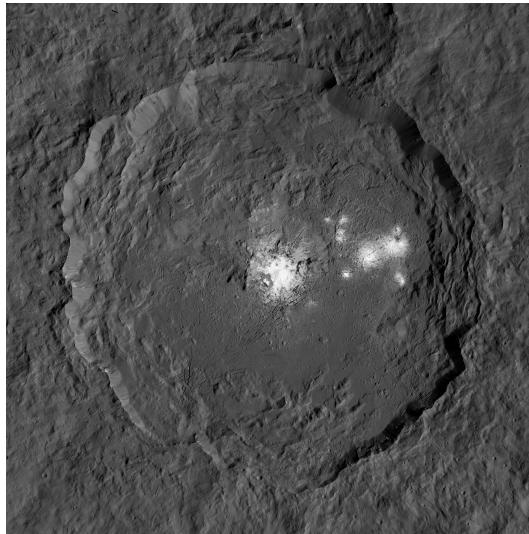


Figure 1: A close-up view of the Occator Crater with its faculae as imaged by the Dawn mission (NASA). The crater is 92 km across (Credits: NASA/JPL-Caltech/UCLA/MPS/DLR/IDA/PSI)

134 contain a significant organic component. This is of interest for two primary reasons. Firstly, during planetary ac-  
135 cretion it has been hypothesised that volatiles and organics were delivered to Earth by carbonaceous chondrites (e.g  
136 Alexander et al. [47]) which subsequently enabled the rise of life. Recent missions to similarly volatile- and organic-  
137 rich bodies such as the comet 67P/Churyumov-Gerasimenko by ESA's Rosetta-Philae have complicated the subject  
138 by suggesting comets were not a major deliverer of these materials [48]. Moreover, the probes of Hayabusa2 (JAXA)  
139 and OSIRIS-REx (NASA) will return samples of carbonaceous asteroids within the next years which will provide new  
140 data. As the largest-known carbonaceous body, further characterisation of Ceres could develop our understanding of  
141 where this body fits in using both meteoritics and returned JAXA/NASA samples, and whether Ceres-class objects  
142 were involved in the seeding of proto-Earth with the components that eventually gave rise to life.

143 Ceres' carbonaceous nature is also of interest because its high volatile content is unusual for its present location.  
144 Ceres' high ammonia content could not have condensed within the Asteroid Belt during planetary accretion because  
145 ammonia is a vapour at expected temperatures during this time [49]. This suggests either Ceres' ammonia and other  
146 volatiles were delivered later or that Ceres itself formed in the outer Solar System before migrating inwards [50]. A  
147 return mission to Ceres could resolve such uncertainties by producing high-precision observations that may further or  
148 preclude particular hypotheses.

149 Taken together, the habitability case for the return to Ceres calls for analysis of both the faculae salts and the more  
150 widespread organics, while the potential role that planetesimals coming from the same reservoir as Ceres had in pro-  
151 viding Earth with life building-blocks may best be studied with a sample of the organics present in the surface rocky  
152 material.

### 153 1.3. The case for Calathus

154 In discovering the faculae and linking Ceres with the wider Solar System, Dawn created as many questions as it  
155 answered. These can be broadly divided into two main categories of interest:

- 156 1. Ceres' spectral features do not match any known meteorite groups, nor can the location of its formation be  
157 pinpointed to a specific region. The question remains as to where and how Ceres formed, and whether asteroids  
158 of similar composition played any role in the delivery of water/organics to proto-Earth.
- 159 2. Ceres appears to contain three of the prerequisites for life: sources of water, carbon, and energy. Ice-rich bodies  
160 like Ceres could represent a widespread, astrobiologically-favourable niche.

161 To understand the composition and evolution of Occator is to understand the inner workings what has been called  
162 a relict — potentially extant — ocean world [51], providing a snap-shot inside not only Ceres but a whole class of  
163 ice-rich bodies. To this end, it is proposed a return mission to Ceres to sample material from Occator Crater. This  
164 would provide invaluable insight into both of these overarching questions, the former of which is in particular an ESA  
165 Cosmic Vision priority, as well as to further the study of a world fascinating in its own right.

#### 166 1.4. Previous and upcoming missions

167 The Calathus mission to Ceres stands on the shoulders of half a century of in situ and sample return missions:

- 168 • The Dawn mission [26] could be considered a precursor or scout mission for Calathus, and provided numer-  
169 ous pieces of evidence supporting the presence of a subsurface cryosphere, as expounded in subsection 1.1.  
170 Returning samples from the faculae salts should help determine its nature and composition.
- 171 • The Cassini mission [52] during its flight through the plumes of Enceladus confirmed the existence of water be-  
172 neath an icy surface. Cassini’s data could be compared with Calathus’ in order to better constrain the conditions  
173 of appearance of subsurface oceans on icy bodies.
- 174 • The Jupiter Icy Moon Explorer (JUICE) mission [53] to the Jovian system will be orbiting the Galilean satellites  
175 by the time Calathus is launched. JUICE will investigate Europa, Callisto and Ganymede, which show strong  
176 evidence for harbouring subsurface water oceans, which is one of the setting for extra-terrestrial life of the icy  
177 worlds. Calathus and JUICE’s results could be treated together to provide knowledge to the appearance of the  
178 conditions of life on the solar system icy bodies.
- 179 • The Exo-Mars mission [54], which will be launched in 2022, aims at studying the biosignatures of past Martian  
180 life. ExoMars and Calathus scientific return could both be handled to answer the question of the appearance of  
181 life in various location in the solar system.
- 182 • Finally, there are multiple lessons to be learnt from the technological aspects of missions hosting landers. The  
183 Rosetta mission with its lander Philae [55] reached the comet 67P/Churyumov-Gerasimenko in 2014, with  
184 the prime objectives of investigating the origin of comets. Rosetta serves as a source of both scientific and  
185 technological inspiration. Philae lander successfully deployed and operated even under adverse circumstances  
186 of harpoon failure on the comet nucleus and thus can be used as a starting point to develop a Ceres lander, by  
187 reinforcing the landing system design where it failed. The lander’s designs are also inspired from missions such  
188 as InSight [56] and upcoming Luna-27 [57].

## 189 2. Science Case

190 Based on the open questions left by the Dawn mission, Calathus is proposing a further exploration of Ceres with  
191 a detail that only a sample return mission can offer. Returning pristine material from Ceres, particularly from the  
192 Occator Crater, and studying it on Earth would provide new insights into fundamental questions related to the origin  
193 and evolution of Ceres and its astrobiological potential. Thus the driving questions addressed by Calathus are broadly  
194 divided into those two categories:

- 195 1. Ceres’ origin and its evolution in the Solar System
- 196 2. Ceres astrobiological potential

197 The Calathus’ scientific questions and the corresponding objectives are described in detail below and summarized in  
198 Table 1 .

199 *2.1. Category 1: Ceres' origin and its evolution in the Solar System*

200 Ceres' spectral features do not match any known meteorite groups, nor can the location of its formation be pin-  
201 pointed to a specific region, leaving the question on where and how Ceres formed open. In this context Calathus  
202 would address the following questions:

203 1.a *What is the nature of Ceres' carbonaceous material?*

204 The physicochemical, mineralogical, and morphological analysis, in situ and on-Earth, of the carbonaceous  
205 material on the Ceres' surface would provide information about its pressure and temperature of formation. This  
206 would constrain the origin of Ceres in the Solar System.

207 1.b *Where did Ceres and other spectrally dark type asteroids form?*

208 Determining the composition of surface material at Ceres would give an insight into Solar System evolution  
209 and reorganization after Jupiter formation. This would constrain the early migration scenario of giant planets in  
210 the Solar System.

211 1.c *What is the nature of the bright material at the Occator's faculae?*

212 The exact composition of the bright spots material is unknown as Dawn's VIR instrument has a limited spectral  
213 range (1-5  $\mu\text{m}$ ). Earth-based analysis are crucial to discretize the chemical species and assess the subsurface  
214 reservoirs composition.

215 *2.2. Category 2: Astrobiology at Ceres*

216 Dawn data revealed the presence of water and localized complex organic molecules on the cerean surface. Both  
217 are essential ingredients for life as it is known on Earth. Whether these organic molecules are original from Ceres  
218 or an exogenous delivery is still to be determined. It is of importance to understand and characterize these organics,  
219 to evaluate the past and present astrobiological potential of Ceres. In this context Calathus would address three main  
220 questions:

221 2.a *Were – or are – the ingredients for life present in the subsurface of Ceres?*

222 The Occator crater is an almost unique place in the Solar System where to easily access and sample pristine  
223 material from subsurface reservoir. By orbital, in-situ and on-Earth characterization of the faculae's material,  
224 the chemical and organic composition of the primordial subsurface reservoir can be investigated.

225 2.b *What role do cryospheres play in the search for life?*

226 The presence of subsurface oceans in other bodies of the Solar System has questioned the concept of habitability  
227 zone as it has been defined. Additionally, the presence on Earth of active deep ocean vents has questioned the  
228 importance of light as a primary source of energy. Therefore, the investigation of the Ceres' cryosphere, even  
229 if no longer active, is an important milestone to study active and relict ocean worlds. The cryovolcanism could  
230 offer a means to expose organics (if present) to water, through the motion of the brine that could promote the  
231 transfer of material from the surface to the subsurface [4] and create flows, fissures, and cracks deep enough for  
232 significant interaction to occur over time. This could promote the formation of more evolved organic species.

233 2.c *Did the main belt asteroids spectrally similar to Ceres contribute to the delivery of Earth's water?*

234 The question of the origin of water on Earth has been discussed mainly based on the deuterium-to-hydrogen ratio  
235 (D/H). In-situ characterization of Ceres hydrogen, oxygen, and nitrogen stable isotopic ratios would provide  
236 additional information about the delivery of water to the Earth, allowing to different proposed scenarios to be  
237 distinguished [58].

238 *2.3. In-situ measurements*

239 In order to address all scientific objectives as well to reduce the complexity of the overall mission, in-situ measure-  
240 ments would be performed, primarily pertaining to the potentially volatile substances. These measurements would  
241 ensure that all objectives of the mission can be achieved regardless of alteration of the volatiles during the return  
242 phase: thus, no active thermal control would be required for the sample and re-entry capsules.

243 The gas chromatography mass spectrometer would analyse in situ the D/H ratio as well as the oxygen and nitrogen

Table 1: Science questions addressed by Calathus

	Science question	Science objective
Ceres Origin and Evolution	What is the nature of Ceres' carbonaceous material?	Investigate the chemical composition of the carbonaceous material.
		Explore the mineralogy and morphology of the carbonate grains.
	Where did Ceres and other spectrally dark type asteroids form?	Map the surface of Ceres.
		Estimate the elemental abundance and isotopic composition (e.g. stable isotopes of oxygen and chromium)
		Estimate the volatile content.
	What is the nature of the bright material at the Occator's faculae?	Identify the mineral composition.
Map the mineral distribution.		
Investigate under what conditions the faculae formed.		
Astrobiology at Ceres	Are the ingredients for life present in the Occator Crater?	Search for the presence of prebiotic and biologically-relevant organic molecules. Characterise the organic material if present.
	What role do cryospheres play in the search for life?	Investigate the physicochemical composition of the subsurface reservoir.
		Search for biosignatures.
Did main belt asteroids spectrally similar to Ceres contribute to the delivery of Earth's water?	Measure hydrogen, oxygen and nitrogen isotopic variations and relative abundances of volatiles on the cerean surface.	

244 stable isotopic ratios of one collected sample, characterise the different isotopic ratios of any volatiles and the relative  
245 abundances of gases exposed during the drilling of the samples. In addition, a detailed mapping of the landing and  
246 sampling sites would be performed, creating topographic maps for an initial characterisation. A thermal infrared map-  
247 per would measure temperature variation of the surface and a surface penetrating radar would be used for selection of  
248 the landing site and analysis of Ceres' geological features.

#### 249 2.4. Sample analysis on Earth

250 In order to fulfil the Calathus' scientific objectives, the following sample analyses are required:

- 251 1. X-ray diffraction (XRD) for determining the mineral or chemical structure of the sample.
- 252 2. Gas-chromatography mass-spectroscopy (GC-MS) for the identification of the insoluble organic phase.
- 253 3. X-ray absorption near-edge structure (XANES) for identifying spatial distributions of organics and minerals  
254 and the link between them.
- 255 4. Electron microprobe for analysing the elemental composition.
- 256 5. Scanning electron microscopy (SEM) for determining the sample microstructure.
- 257 6. Thermal ionization mass spectrometry (TIMS) for calculating the age of the components, by calculating ratios  
258 of radioactive isotopes.

259 All mentioned methods require large, massive and extremely high precision instrumentation, which is not feasible to  
260 accommodate on a spacecraft. Thus these measurements would be carried out on the samples after their retrieval on  
261 Earth. Additionally, a percentage of the samples would be stored and would provide material for future generations  
262 of scientists to use methods and techniques not yet invented.

263 The main priority of the sample return is the retrieval of the white carbonate material from the Occator faculae. As  
264 dark coloured organic matter is ubiquitous on the surface [59], it is highly likely that it would also be present at the  
265 landing site. In the unlikely case of the sample containing exclusively white material, the majority of the scientific  
266 questions could be answered.



### 267 3. Mission requirements

268 A system engineering approach has been used by employing the concurrent design software Open Concurrent  
269 Design Tool (OCDT) from ESA [60] which leads to a Phase 0 study of a sample return mission to Occator crater.  
270 Requirements have been identified at system and subsystem level but, for the sake of brevity, only system driving  
271 requirements are listed in this section. The driving requirements are:

- 272 1. The mission shall perform a sample return of at least a total of  $4 \text{ cm}^3$  of bright material from Ceres to ensure  
273 there is enough mass to perform the minimum necessary analysis on Earth.
- 274 2. The sampling mechanisms shall be capable of removing the upper 5 mm of the surface and sampling from  
275 below this depth so as to avoid to sample material from the the near subsurface which may be contaminated by  
276 space-weathering [61].
- 277 3. Contamination of the surface of Ceres shall be limited to  $180 \text{ ng/cm}^2$  of hydrazine during descent as in the  
278 OSIRIS-REx mission [62]
- 279 4. Four samples of  $4 \text{ cm}^3$  shall be collected and returned to Earth in order to maximise the amount of analysis that  
280 can be performed on Earth.
- 281 5. At least one additional sample shall be collected and analysed in-situ.
- 282 6. The lander shall be able to cope with boulders and surface features up to diameter 0.6 m. This requirement is  
283 driven by the small lander size.
- 284 7. The Calathus system shall support the selection of sampling locations based on visual inspection.
- 285 8. The samples shall not be contaminated with terrestrial material or organics.
- 286 9. The conditions in the interior of the sample capsule shall be monitored during return phase, re-entry and col-  
287 lection. It must be noticed that in this paper the design of the re-entry capsule itself is not addressed. Thus, the  
288 monitoring system inside the capsule is not expounded.
- 289 10. The orbiter should characterise Ceres surface with a resolution of 1.1 px/m to identify the correct landing site  
290 and to provide scientific and contextual information for the sample analysis

291 These requirements influence what are considered to be the most critical part of the design: the sampling operation  
292 (items 1, 2, 5 and 7), the sampling mechanism (items 2, 4, 5 and 7), the lander descent (items 3 and 6), the planetary  
293 protection (items 3, 8 and 9), and the landing site selection (item 10).

### 294 4. Mission profile

295 The goal of Calathus mission is to return a sample from Ceres. The spacecraft Calathus consists of four segments:  
296 the orbiter, the sample canister, the propulsion platform and the surface module. The latter three parts comprise the  
297 lander Piazzzi.

298 The mission phases are summarised in Figure 2 and detailed in the following sections.

#### 299 4.1. Launch requirements

300 The Calathus mission would begin with a launch from Kourou, French Guiana, using the Ariane 64 rocket. The  
301 spacecraft's wet mass at launch is 5780 kg, and the dimensions (see Table 5 at the end of the article) allows for a dual  
302 launch configuration. The targeted  $\Delta V$  is 10.6 km/s in the Earth inertial frame, which allows for a good start on the  
303 trajectory to Ceres.

#### 304 4.2. Interplanetary Trajectory

305 Two different interplanetary orbits had to be defined for this mission. The initial connects the Earth to Ceres: this  
306 trajectory was designed using low-thrust propulsion and also leveraging a flyby to Mars for gravity assist. Since this  
307 is a sample return mission, the return trajectory is also optimized and analyzed using an analytic-based method. For  
308 the return case, a relatively high infinite velocity at the Earth is allowed, since most of the remaining energy can be  
309 dissipated in the Earth's atmosphere during the re-entry trajectory.

310 The outbound orbit is found by optimizing the whole trajectory in a global optimization framework. Specifically, a  
311 local optimizer of the ESA's global optimization toolbox PaGMO was used [63, 64]. This has allowed an orbit that

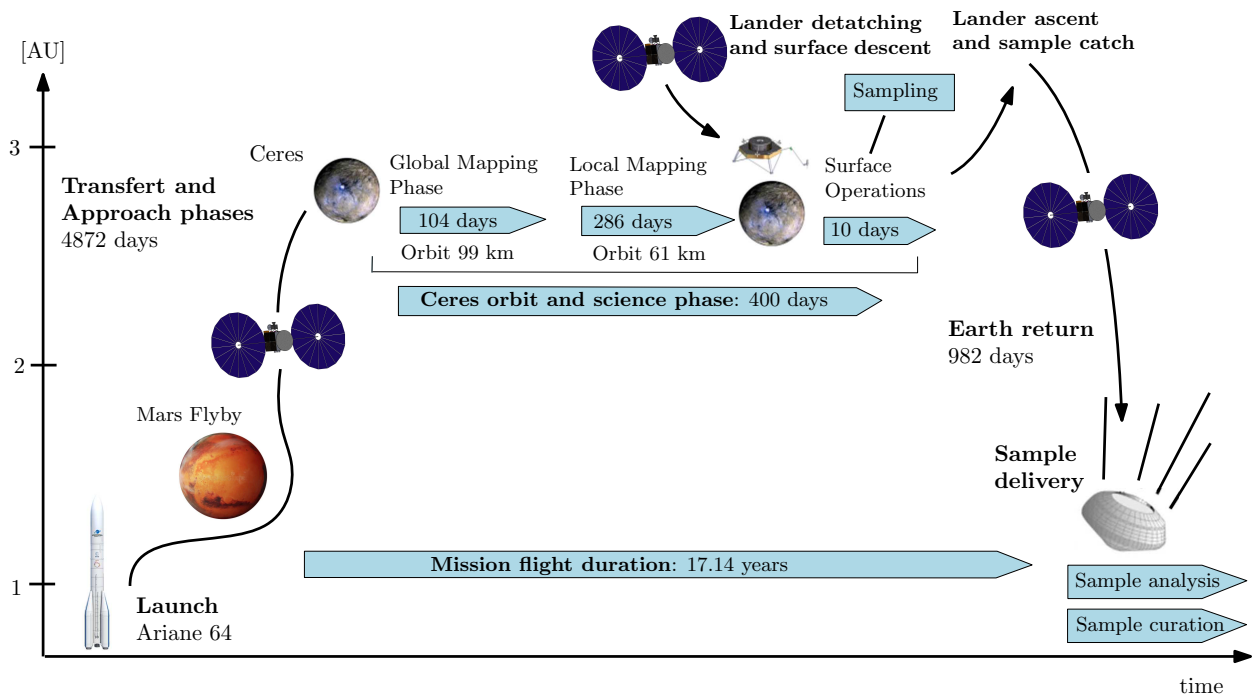


Figure 2: Visualisation of the mission phases of Calathus.

312 possibly minimizes the propellant consumption to be found, while still fulfilling the mission and system requirements.  
 313 This orbit has a departing date: of the 29<sup>th</sup> of April 2031. After four revolutions around the Sun and a journey that lasts  
 314 nearly 4872 days, the spacecraft then reaches Ceres on the 30<sup>th</sup> of August 2044. In Figure 3 the three-dimensional  
 315 trajectory in the Sun-centered ecliptic reference frame and its two-dimensional projections are shown. During its  
 316 journey, the spacecraft performs a flyby of Mars (for which it was designed and optimized), gaining a change in  
 317 velocity ( $\Delta V$ ) of 2.7 km/s. Also, the orbit shows a spiral-like shape that is typical for low-thrust orbits.  
 318 For the inbound trajectory, an analytical representation of low-thrust trajectory has been employed, which has allowed  
 319 an inbound trajectory with a low time of flight, a feasible thrust profile and re-entry velocity, and a reasonable infinite  
 320 velocity at Ceres to be executed. The implemented technique for finding such a orbit consists of a shape-based method  
 321 to first derive an analytical formulation of the trajectory: from the analytical expression of the trajectory, quantities  
 322 (such as acceleration, velocity, thrust, mass consumption, etc.) can then be derived to investigate the feasibility and  
 323 quality of such orbit. The shape-based exponential sinusoid method was used in this paper [65, 66, 67]. The trajectory  
 324 resulting from this analysis is presented in Figure 4. As shown, the spacecraft reaches the Earth from Ceres (after  
 325 having studied the dwarf planet's surface for 400 days) in only one revolution. In particular, the time of flight of this  
 326 trajectory is 2.69 years: this means that the spacecraft would leave Ceres on the 4<sup>th</sup> of October 2045 and it would  
 327 reach the Earth on the 11<sup>th</sup> of June 2048. The spacecraft arrives at Earth with an infinite velocity of  $v_{\infty} = 5.4$  km/s,  
 328 which allows a re-entry velocity (at 120 km altitude with respect to the Earth surface) of 12.3 km/s. The required  
 329 initial  $\Delta V$  at Ceres for the spacecraft to be injected in such a orbit (i.e., for reaching the required escape velocity at  
 330 Ceres) is 0.4 km/s. It is important to highlight that the 10 Earth days time window for surface operations at Ceres does  
 331 not take into account anomaly procedures. In future studies, if a new timeline is set-up, it might be needed to iterate  
 332 on the design of the inbound trajectory.

### 333 4.3. Trajectory at Ceres

334 The trajectory at Ceres aims at fulfilling the previously-mentioned scientific and mission requirements by choosing  
 335 the correct orbit for the spacecraft. For the sake of this study, in this preliminary design all orbits are considered circular  
 336 and the gravity field of Ceres considers only the term  $J_2$  [27], i.e. the flattening, in order to consider the precession  
 337 of the ascending node of the orbit. All orbital operations around Ceres are performed with chemical propulsion. This

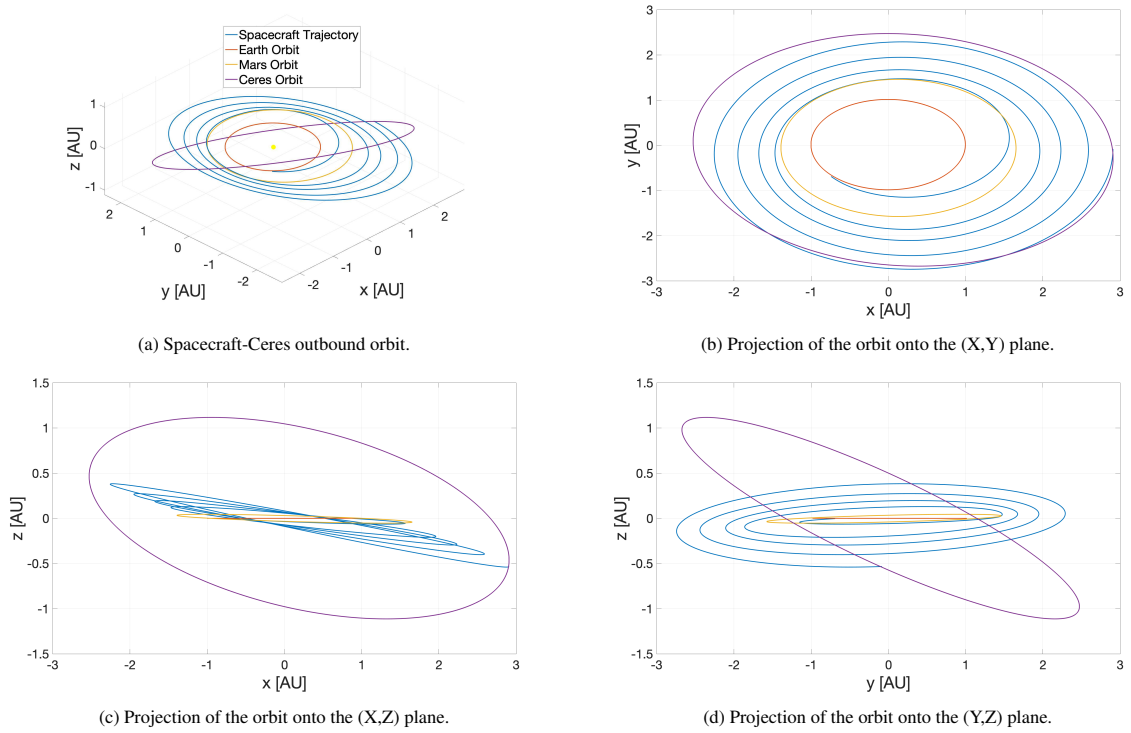


Figure 3: Spacecraft trajectory and its projections in the (X,Y,Z) ecliptic reference system centred in the Sun's barycenter.

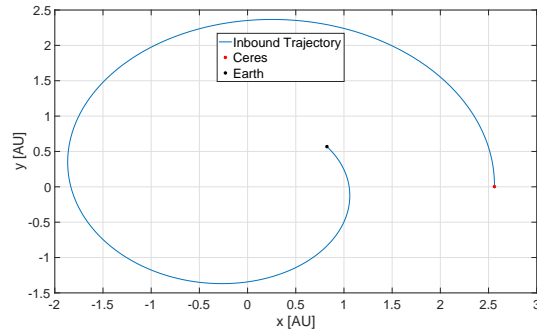


Figure 4: Inbound trajectory expressed in a plane that has the x-axis collinear to the starting position of Ceres and centered in the Sun.

338 has several advantages: it reduces costs related with xenon; it improves the gravity field determination strategy as  
 339 longer arc without firing can be exploited; and it reduces the complexity in the orbit determination process. The oper-  
 340 ations at Ceres are separated into four different phases that correspond to different operational altitudes - given with  
 341 respect to the reference Digital Terrain Model (DTM) spheroid radius (470 km) - and inclinations:

- 342 1. The insertion procedure on the highest orbit around Ceres from the interplanetary trajectory. It is assumed  
 343 that the B-plane has been correctly targeted during approach thanks to trajectory correction manoeuvres. The  
 344 targeted orbit, labelled High-Altitude Mapping Orbit (HAMO), is at an altitude of 99.08 km with respect to  
 345 the surface and an inclination of  $95^\circ$ . The altitude has been chosen to ensure that the camera resolution fulfils  
 346 the requirement of 1.1 m/px for the global mapping and to complete, thanks to  $J_2$ -induced precession of the  
 347 node, 662 orbits in 221 Ceres days, i.e. 83.5 Earth days, among which 22 cover the Occator crater. To allow

348 the transmission of the collected data and to ensure a better global coverage, as the other spherical harmonics  
349 coefficients that have not been considered could perturb the orbit, 20 days are added to this phase of the mission.  
350 The total duration is 104 Earth days. The  $\Delta V$  necessary to perform the insertion is  $167 \text{ m s}^{-1}$  and considers the  
351 circularization of the interplanetary orbit and a back-up change of plane of  $10^\circ$  if the B-plane is not targeted  
352 correctly.

- 353 2. The local mapping of the crater to characterise the possible landing sites and the detailed geomorphology of  
354 Occator's crater. The orbit, labelled Low-Altitude Mapping Orbit (LAMO), is at an altitude of 61.25 km with  
355 an inclination of  $95^\circ$ . Lower orbits have been considered too affected for higher terms of the gravity field to be  
356 operational. The inclination is chosen to minimise the propellant used to pass from HAMO to LAMO. This orbit  
357 allows a resolution of 0.6 m/px. By considering that 0.6-m boulders are detectable with a resolution of 0.3 m/px,  
358 only boulder of diameter of 1.2 m can be detected. Boulders smaller than 1.2 m are detected during descent by  
359 the autonomous hazardous detection and avoidance system. Smaller hazards would be avoided and managed  
360 by the active and controlled descent of the lander as a closest orbit would be perturbed too much by the gravity  
361 field. Similarly to the HAMO, the LAMO is chosen because of the precession of the node that allow Ceres to  
362 be mapped with the previously-mentioned precision in 1211 orbits in 365 Ceres days, i.e. 138 Earth's days. In  
363 order to use the whole scientific suite, the precession is done twice with some margin and this operational phase  
364 of the mission lasts 286 Earth's days in order to ensure correct data storage and communication. During this  
365 phase about 80 orbits are flown above the Occator Crater, while others are flown to map and characterise other  
366 interesting sites, as the Ernutet crater, with a lower resolution than the Dawn mission. The  $\Delta V$  to move from  
367 the HAMO to LAMO, including the inclination change, is  $69.50 \text{ m s}^{-1}$ .
- 368 3. The release of the lander is performed at an altitude of 20 km over the chosen landing site, i.e. Occator crater.  
369 The required  $\Delta V$  is estimated to be  $13.84 \text{ m s}^{-1}$ .
- 370 4. The orbiter then increases its altitude to 109.16 km and changes its inclination to  $150^\circ$  in order to put itself on  
371 the Surface Operation Orbit (SOO) where two slots of communication are available each Ceres day. The  $\Delta V$   
372 required for the change of plane and to reach the SOO altitude from the lander release altitude is 28.48 m/s.  
373 Each slot of communication lasts about 30 minutes long which assures the lander operations would be planned  
374 and executed on time.

#### 375 4.4. *Descent and in-situ operations*

376 Once the Piazzoli lander is released from the orbiter, it performs an active descent to correctly target the landing  
377 location. The lander is designed to be static and operate from the landing position to collect samples. The active  
378 landing is chosen mainly for two reasons. Firstly, the active descent allows hazard detection and avoidance thanks  
379 to the Guidance Navigation and Control (GNC) suite on board of the Piazzoli lander. Secondly, the control scheme  
380 can actively adjust the orientation of the landing platform to ensure the correct operations of sample selection and  
381 collection. The descent trajectory is computed with a ZEM/ZEV guidance planning algorithm and lasts about 26  
382 minutes by using a  $\Delta V$  of  $429.3 \text{ m s}^{-1}$ . Moreover, the landing gear is designed to be able to damp for about  $2.5 \text{ m s}^{-1}$   
383 impact speed and has heritage from the Mars and Moon Landing with a TRL of 4.

384 Once on the surface, the in-situ operations start. The nominal concept of operation aims to collect five different  
385 samples from the surface thanks to a sampling mechanism that is placed at the end of a robotic arm (see the following  
386 sections for configuration and figures) that is observed from a camera placed on the same arm. The five samples are  
387 collected from five different sites around the landing site which are reachable with the robotic arm and safe to sample  
388 for the drilling mechanism. The camera is a fundamental instrument for science and operation of the Piazzoli lander on  
389 the surface as it ensures not only in-situ images to choose the correct sampling sites, but helps engineers to observe  
390 the sampling procedure and ensure it is carried out correctly.

391 The concept of operation for sampling is divided in the following steps:

- 392 1. After landing, Piazzoli takes a series of 12 images covering the area accessible to the sampling arm.
- 393 2. Descent images, housekeeping and landing images acquired by the lander's camera are down-linked through  
394 the orbiter to Earth, where the status of the rover is assessed. Drill sites are selected based on the post-landing  
395 images.
- 396 3. Commands to collect sample 1 are sent to and executed by the lander.

- 397 4. Post-drill images and housekeeping data are down-linked to Earth to assess the collection of sample 1 and  
398 possibly reevaluate drilling sites selection.
- 399 5. If the collection of sample 1 is successful, commands to collect sample 2 are sent to and executed by the rover.
- 400 6. Steps 4 and 5 are repeated for each sample.

401 The nominal time of operation is 10 Earth days, i.e. 26 Ceres days. This implies 52 slots for communication  
402 which allows for ground-based decisions before each sampling operation. Several attempts may be necessary before  
403 the first successful drill; this would result in the repetition of steps 3 and 4. This timeline has been designed without  
404 considering sampling system failures or anomalies. Future studies should define a more robust operational scenario  
405 which must consider wider time margins. This implies possible changes in the overall design on lander power system  
406 and inbound trajectory as mentioned in the respective sections.

407 The drilling mechanism is composed of a penetrating drill and a brushing mechanism, as explained in Section 5.2.3,  
408 that is used to remove the uppermost space-weathered layer of the surface that may have been contaminated by the  
409 engines' exhaust, and a drill with different power increments to collect the samples. Once the sample is collected, the  
410 arm places it into a basket in the bus. The process is repeated four times for as many samples, with a fifth repetition  
411 placing a sample into the on-board mass spectrometer to determine Ceres' hydrogen, oxygen, and nitrogen stable  
412 isotopic ratios and relative abundances of volatile subsurface material. This is done in order to ensure the science  
413 margin even in case of failure during sample canister catching, outbound interplanetary trajectory or reentry on Earth.  
414 When finished, the arm performs a 360° horizontal rotation to capture a panorama from the landing site.

#### 415 4.5. *Sample canister catching*

416 The lander uses the same algorithm, i.e. the ZEM/ZEV guidance planning algorithm, to design its ascent trajectory.  
417 In this case, a trajectory from the ground to the SOO is considered, which lasts 34.17 minutes and consumes 499.54  
418 m s<sup>-1</sup>. The ascending module is then put on the same orbit as the orbiter, where catching operation can start. This is  
419 divided into two different phases: the cooperative rendez-vous and the sample canister catching.

420 The cooperative rendez-vous starts with a large distances between the orbiter and the ascending module, where the  
421 two modules cooperatively and autonomously reduce their relative distance thanks to the autonomous GNC system,  
422 outlined in the Section 6.9. It must be noted that the rendez-vous is cooperative as both modules are actively controlled  
423 and can modify their attitude and position with the use of thrusters and reaction wheels. When the nominal distance  
424 and correct attitude are reached, the ascending module releases the sample canister in the direction of the orbiter's  
425 collecting mechanism, which draws inspiration from the Mars Sample return mission [68]. The catching phase starts.  
426 The orbiter tracks the sample canister thanks to LIDAR and vision-based navigation until it is captured from the  
427 capture cone and it is then placed in the reentry capsule to be stored and safely brought back to Earth.

#### 428 4.6. *End-of-Life disposal and curation facility on Earth*

429 Ceres is classified with respect to planetary protection concerns. As is it a sample return mission, it is classified as  
430 a class V mission [20]. The COSPAR comity has established six criteria to decided if a mission should be restricted  
431 or unrestricted [20]. Actually, five of the six criteria could be discussed at a global level: there may have been liquid  
432 water and metabolically useful energy sources on Ceres in the past, quantity of organics have been detected by Dawn,  
433 it is not certain that Ceres has been subjected to extreme temperatures and no proof of a natural influx from Ceres to  
434 Earth exists at the present time. Finally, as shown in Castillo-Rogez and Brophy [69], the ionization dose received by  
435 each site on the Ceres's surface is the critical point for the sub-classification restricted/unrestricted. Ceres is an old  
436 object and in average, the organic matter present on the surface has been exposed to cosmic rays for several million  
437 years, which assure the sterilization of the surface : "the sterilization is achieved after about 1 My for superficial  
438 material down to 10 cm" according to Castillo-Rogez and Brophy [69]. On the opposite, salts from the Occator  
439 faculae have been exposed to cosmic rays more recently and given the uncertainty about the dating of the site, the  
440 NASA pre-decadal report [69] concluded that the restricted classification is required for the sample return missions  
441 from the Occator faculae. Because of this classification, it is required to understand how the different modules orbiting  
442 or located on the surface of the dwarf planet are disposed.

443 The ascending module is located on an non-impacting orbit around the dwarf planet consistent with the end-of-life  
444 orbit of the the Dawn spacecraft, for at least 20 years with a probability of 99%, and for at least 50 years with  
445 probability of 95% [70]. The lander instrument suite would remain on the surface.

446 This also means that everything that has been in contact with Ceres must be tightly contained or sterilised before and  
447 after re-entry. Once the sample has landed on Earth, it would be retrieved and brought to the European Curation of  
448 Astromaterials Returned from the Exploration of Space (EURO-CARES) facilities in the UK [71], via refrigerated  
449 transport at temperatures below -20°C. At the EURO-CARES facilities, the basket and two of the four sample capsules  
450 would be opened in a refrigerated and atmosphere controlled containment chamber. The chamber would be built  
451 according to Planetary Protection standards to avoid any contamination of the sample by terrestrial life, contamination  
452 of Earth by cerean material, or chemical alteration of the sample. When analysis has mapped any risk and ensured  
453 there is no danger of contamination, the opened sample material would be characterized and catalogued, before half  
454 of it is distributed to laboratories after a review of their proposed utilization. The other half (i.e. the two remaining  
455 capsules) would be preserved for the future generation.

## 456 **5. Payload**

457 The main scientific goal of this mission is to return to Earth a sample of the Occator Crater faculae for high-  
458 precision laboratory analyses. A suite of scientific instruments is necessary to identify the best landing site, to monitor  
459 the descent and drilling phase, and to collect geological and physical information about Ceres and its environment. The  
460 orbiter would carry a surface-penetrating radar, a thermal infrared mapper, and a narrow angle camera. These three  
461 instruments would perform global measurements needed for both landing site selection as well as contextualization  
462 of the sample return measurements.

463 The lander would be equipped with a gas chromatograph mass spectrometer, descent cameras, an arm camera, as well  
464 as a drilling and sampling systems. The cameras would provide geological context for sampling site selection as well  
465 as support for sampling operations, while the mass spectrometer would yield the first ever in-situ measurements of the  
466 composition of an airless body surface.

467 The presence of scientific instruments on both the orbiter and the lander mitigates the risk of single point of failure  
468 since they fulfil the scientific requirements defined in Section 2 to address the scientific objectives of the mission.

### 469 *5.1. Orbiter*

470 The Calathus orbiter's scientific payload would include three instruments: a narrow angle camera, a thermal  
471 infrared mapper, and a radar.

#### 472 *5.1.1. High Resolution Narrow Angle Camera*

473 The orbiter would include a high resolution Narrow Angle Camera (NAC), whose objectives would be to observe  
474 and map the surface, providing information about its appearance and morphology. The mapping phases would help  
475 finding a suitable landing site.

476 The Dawn mission mapped a limited area of Ceres with a resolution up to 3.3 m/px achieved on its closest fly-by. The  
477 camera on the orbiter would be build on heritage from the OSIRIS Narrow Angle Camera on board of the Rosetta  
478 spacecraft [72]. OSIRIS consisted of an off-axis mirror system equipped with backside illuminated CCD detectors,  
479 with a field of view (FOV) of 2.2 degrees, comprising 2048 x 2048 pixels with a pixel size of 13.5  $\mu\text{m}$ , and an  
480 instantaneous field of view (IFOV) of 18.6  $\mu\text{rad}$  (3.8 arcsec) per pixel [72]. Since the Calathus mission would be more  
481 than ten years into the future, the CCD from the NAC on-board Rosetta would be replaced with a more modern one  
482 with 4096 x 4096 pixels. It would allow the Occator Crater to be mapped with a spatial resolution of about 0.57 m/px  
483 from a distance of 61 km during the low-altitude mapping phase. Surface features of down to 1 m would be resolved  
484 and images taken during that phase would be used to select the safest landing site. The resulting images would be  
485 improved by a factor six compared to the Dawn's highest-resolution images. Shape reconstruction techniques, such as  
486 stereophotoclinometry (SPC) and stereophotogrammetry (SPG), would help achieving subpixel precision by merging  
487 different phase angle images [73, 74].

#### 488 *5.1.2. Thermal Infrared Mapper*

489 Thermal mapping of Ceres would provide information on the local and global physical properties of Ceres, such  
490 as surface porosity and grain size distribution.

491 A thermal infrared camera, similar to the Thermal InfraRed imager (TIR) designed for the Hayabusa2 mission [75],

492 would yield thermal emissions maps of Ceres. TIM observes in the wavelength range 8 to 12  $\mu\text{m}$ . With a field of  
493 view of 16 deg  $\times$  12 deg, the TIM (Thermal Infrared Mapper) would be able to characterise the thermal inertia of  
494 the landing and sampling site as well as other regions of interests. As the TIM measurements require relatively little  
495 power and yield light weight data products (less 200 kb/image), it can be operated along with the NAC during the  
496 mapping phase, yielding a global thermal inertia map of Ceres at both daytime and nighttime. TIM is meant to support  
497 landing site selection operations by providing information on the global surface roughness while also helping to fulfil  
498 several science objectives such as characterising surface properties and mapping Ceres' mineral distribution.

### 499 5.1.3. Radar

500 To investigate the formation of Ceres' faculae, structural information about the cerean subsurface is required.  
501 The radar's data would provide the vertical context of the sampling site, which would help in selecting the most  
502 appropriate landing site and understand the sample's analyses. Moreover, probing the surface down to several tens  
503 of meters, with a resolution a few meters, would shed some light on how these faculae are formed, by emphasising  
504 embedded volcanism features, fractures and possibly the salt-rich waters if the radar's waves penetrate at a sufficient  
505 depth. The Calathus orbiter would therefore carry a radar inspired by the SHARAD radar designed for the MRO  
506 mission (NASA) [76]. This radar would be imaging the first tens of meters of the subsurface minimum, with a vertical  
507 resolution of few meters. These two parameters could be evaluated with a better precision by testing the radar's  
508 behaviour along with analogues of the subsurface of Ceres, either by direct experiments (as described in [77] for  
509 Mars) or by simulations (as described in [78] for Europa). If the bright material observed by Dawn is brought up from  
510 the subsurface of Ceres, topographic images of the subsurface area below the sampling site (as well as other faculae  
511 featuring craters) might be a key element to support such theories.

## 512 5.2. Lander

513 The Piazzoli lander would consist of an hexagonal instrument platform carrying cameras and a mass spectrometer.  
514 The lander would also include the drilling system, the sample canister basket, and the ascent module.

### 515 5.2.1. Cameras

516 The lander would include two cameras to provide geological context for the sample and support ground-based  
517 decisions about the sampling site. The first would be mounted on the lander body underneath the top deck, and would  
518 be built on heritage from the Lander Imaging System (ROLIS) on board the Philae lander. This instrument consists of  
519 a miniaturised CCD camera and four independent arrays of light emitting diodes (LEDs) in visible and near-infrared  
520 wavelength to illuminate the field of view [79]. This field of view is large of 25°  $\times$  25° with 2048  $\times$  2048 pixels:  
521 the camera can thus provide a pixel size of 0.15 m at a distance of about 700 m. It would acquire images during the  
522 descent of the lander towards Ceres, yielding geological context crucial for scientific investigations but also serving  
523 as a monitor of the descent phase. This camera would allow hazardous boulders from about 700 m of altitude to be  
524 recognised, which gives margin for safe landing.

525 The second camera would be mounted on the robotic arm of the lander. The camera is the same as on board the  
526 InSight Mars lander and features a resolution of 0.82 mrad/px [80]. The objectives of the camera are monitoring the  
527 location of the drilling system, and investigating the geological and physical properties of the landing and drilling site.  
528 After landing, 12 images forming a panoramic shot of the area would be used to determine the location of the exact  
529 landing site. One *monitoring* image of the first sampling site would be taken after the first drilling and downlinked  
530 to ground. If the first drilling is successful, the subsequent drillings would take place and their monitoring images  
531 would be downlinked after all drillings commands have been executed. These detailed images can reveal the granular  
532 texture of Ceres's surface down to the cm scale, allowing fragments of material of diverse shapes and sizes to be  
533 characterised. The size-frequency distribution and shape analysis of these fragments would help to investigate the  
534 origin of these elements [81].

### 535 5.2.2. Mass Spectrometer

536 In situ analysis of one collected sample would be performed on the lander by a gas chromatography mass spec-  
537 trometer similar to the one carried by Philae to the comet 67P/Churyumov-Gerasimenko, Ptolemy [82]. The mass  
538 spectrometer would measure the isotopic composition of volatiles present in the collected sample, thus assuring a

539 significant science return in case the other collected samples are not returned to Earth intact. Namely, a measurement  
540 of particular interest for the science case is the D/H ratio of the water found in Ceres material, which may provide  
541 insight as to whether Ceres-type bodies played a role in the delivery of water to Earth.

### 542 5.2.3. *Drilling and Sampling Systems*

543 To satisfy the scientific requirements of the mission, four samples of about 4 cm<sup>3</sup> of material have to be collected.  
544 One additional sample of 0.5 cm<sup>3</sup> would be analysed by the on-board mass spectrometer to investigate the composition  
545 of the surface. Several requirements must be verified during sampling. Firstly, the mechanism temperature during  
546 sampling should remain below -20 °C as to preserve the volatile materials. Secondly, the sampling mechanism should  
547 drill different types of soils due to the lack of knowledge of Ceres' surface composition: from solid terrain with  
548 compressive strength up to 20 MPa to loose material with different adhesion values. Finally, the system should  
549 remove the upper layer of the cerean soil up to 5 mm to collect pristine material not affected by space weathering.  
550 The drilling and sampling system would be composed of the four following instruments: a hammering drill to collect  
551 samples, a camera to provide feedback, a mechanical grinding device to clean the sampling area and a manipulator to  
552 operate the instruments. The hammering drill would take heritage from the CHOMIK instrument carried by Phobos-  
553 Grunt [83]. This instrument would be based on the accumulation of electric energy which is then released from an  
554 electromagnetic system in form of strokes to create the torsional and linear movement of the drill [84]. A detachable  
555 sampling container, made of hardened titanium with diamond inserted at the bottom, also plays the role of a drilling  
556 bit [85]. The length of the cylindrical sampling container would be of 5 cm in order to ensure the required 4 cm<sup>3</sup>  
557 of material per sample. The 2-meter long manipulator would be based on already available systems with profound  
558 space heritage, like InSight [86], or technologies matured for flight, such as the Phobos-Grunt [87] manipulator (in  
559 Figure 5). Moreover, the mechanical grinding device would be made with bristles made of titanium and a motor would  
560 be in charge of the grinding movement.

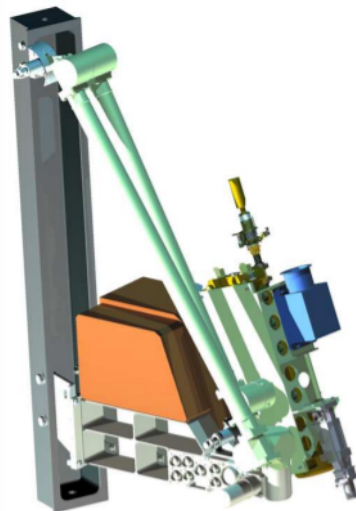


Figure 5: The Phobos-Grunt manipulator (see [85])

## 561 6. Spacecraft bus and lander design

562 The Calathus spacecraft, in Figure 6, would consist of a box with dimensions 4.75 m × 4.27 m × 4.27 m. It would  
563 include a rendez-vous system, a high-gain antenna, two 9.5 m size solar panels on the orbiter. The lander is battery  
564 powered and attached to the orbiter until release. The final launch configuration would fit the allowed fairing volume  
565 as shown in Figure 7.



566 *6.1. Mechanical Subsystem and Mechanisms*

567 The orbiter structure has been designed to allocate all the instruments and the propellant tanks. A central cylinder,  
 568 located in the bottom part of the orbiter, ensures the correct attachment on the launcher interface ring which increases  
 569 the stiffness to launch loads. The propellant tanks are designed to allocate the needed propellants, i.e. the xenon and  
 570 the chemical. The two central tanks, in Figure 8, are designed in titanium to allocate the xenon required for the ion  
 571 thrusters; whereas the four circular tanks are used for the chemical bipropellant propergol storage. The pressurising  
 572 system is not shown in Figure 8. The orbiter structure is composed of Carbon-Fiber-Reinforced Polymer (CFRP)  
 573 sandwich panel to ensure rigidity and low weight. Stresses caused by launch are distributed on the structure thanks  
 574 to the central cylinder where the xenon tanks are, as presented in Figure 8. The structure material is widely used in  
 space missions, with high TRL and heritage from LISA and Dawn spacecraft.

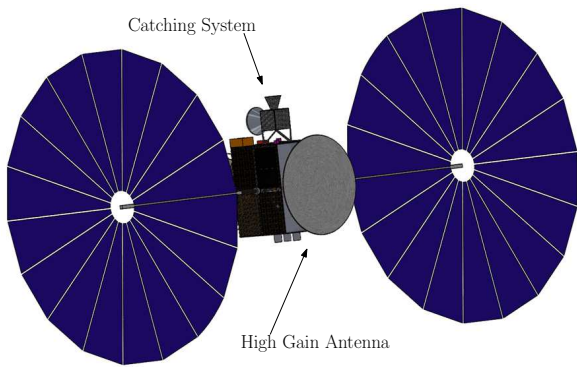


Figure 6: The orbiter after the deployment of the solar panels

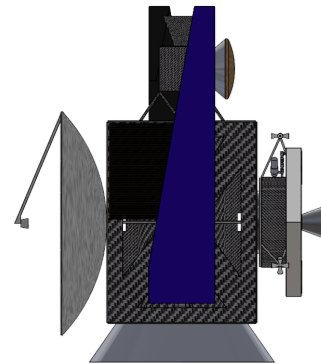


Figure 7: The orbiter closed as in the Ariane 64's fairing

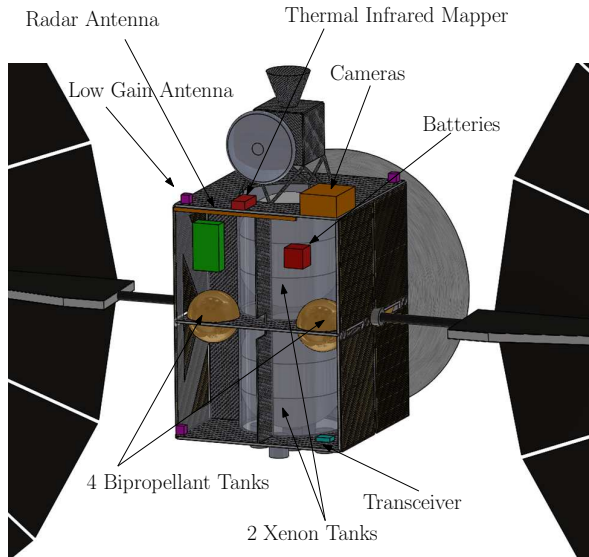


Figure 8: The allocation of the orbiter components in the orbiter

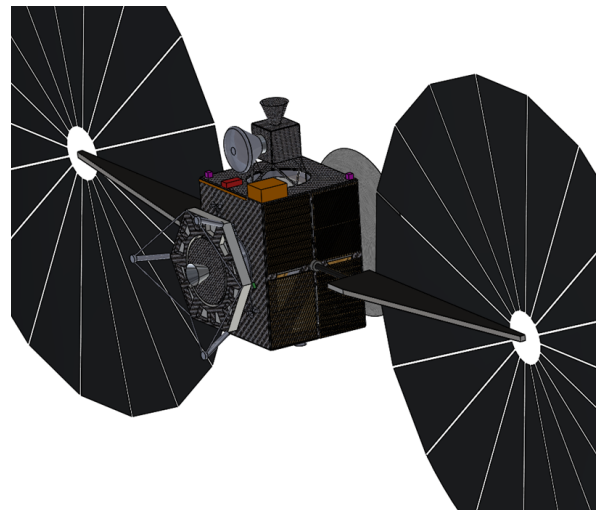


Figure 9: The lander attached to the orbiter structure

575 As shown in Figures 8 and 9 the catching system is on the top part of the orbiter, where instrumentation and cameras  
 576 are placed, and the lander is placed on the side. Figures 10 and 11 show the top and bottom view of the lander,  
 577 designed with CFRP sandwich panels while a beam structure is used to ensure a light module that minimises the fuel  
 578 consumption during ascent whilst ensuring the load is distributed during landing. The instrument platform is designed  
 579 to have holes where instruments, such as the mass spectrometer and the camera, are located to assure the thermal  
 580 requirement and to reduce the mass of the overall structure. In Figure 12, the three main subsystems of the Piazzini  
 581

582 lander are shown. In particular, it is important to note the ascending module configuration where the attitude thrusters,  
 583 the central manoeuvring nozzle and the hydrazine tanks are shown.

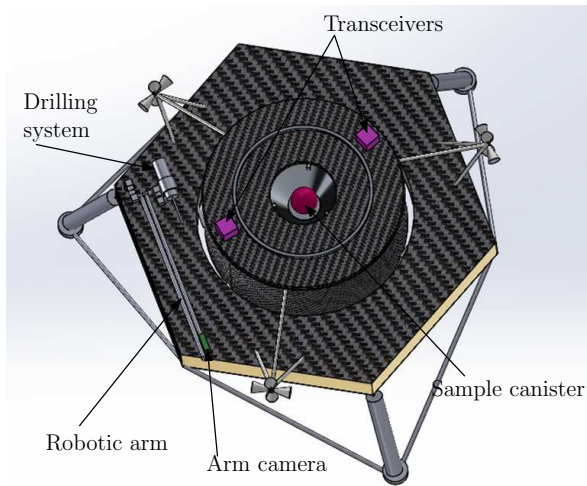


Figure 10: The top view of the lander

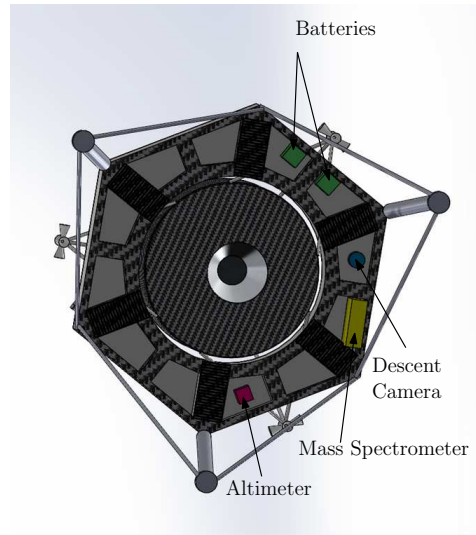


Figure 11: The bottom view of the lander

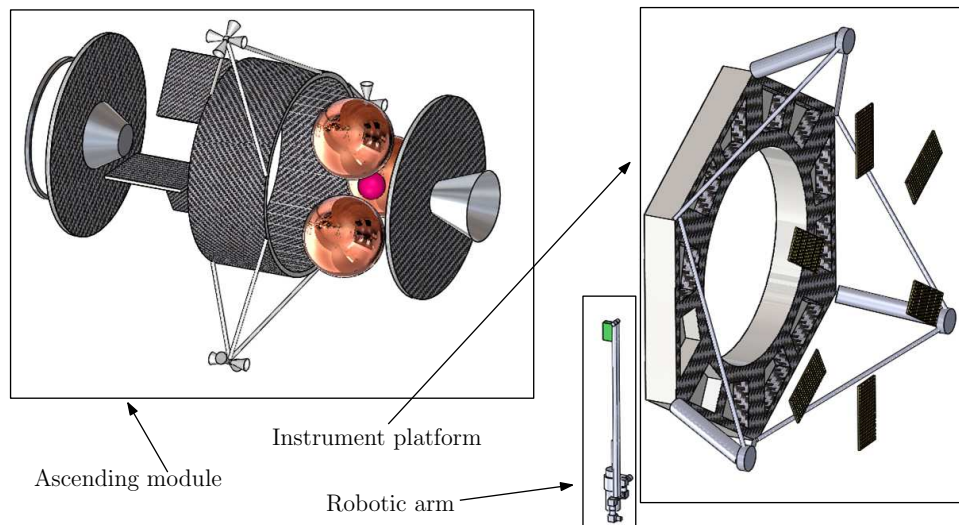


Figure 12: The allocation of the lander components in the lander

584 **6.2. Propulsion Subsystems**

585 Three independent propulsion systems are required for the mission: high specific impulse ion thrusters for the  
 586 Earth-Ceres-Earth transfers, a bipropellant NTO/MMH (nitrogen tetroxide/ Monomethylhydrazine ) thruster for im-  
 587 pulsive manoeuvres close to Ceres, and a hydrazine monopropellant thruster for the lander. Using current technology,  
 588 about 2 tons of xenon would be needed if QinetiQ T6 ion thrusters were used [88], and about 900 kg of NTO/MMH  
 589 would be required using an ArianeGroup S400-15 thruster. As the required propellant for both the ion thruster and  
 590 the bipropellant thruster is so high, it would be interesting to qualify QinetiQ T6 at an operation point of higher  $I_{sp}$ . A  
 591 dedicated high  $I_{sp}$  ion thruster could also be considered for the mission, as was done for the BepiColombo spacecraft

592 where it led to a reduction in xenon mass to 580 kg. This improvement would be justified by the fact that reducing the  
593 xenon mass directly influences the cost of the mission. In fact, the annual world-wide production of xenon is about 53  
594 tons and the use of 2 tons for the mission implies high cost.

595 The lander propulsion system uses hydrazine as propellant which is stored in 3 tanks placed in the ascending module  
596 (see Figure 12). A central thruster is used for the ascending and descending trajectory control.

597 Both the orbiter and the lander use helium for pressurisation of the tanks (2.7 and 0.4 kg respectively) and a cluster  
598 of 12 thrusters for attitude control which use hydrazine or the bipropellant NTO/MMH for the lander and orbiter  
599 respectively.

### 600 *6.3. Communication Subsystem*

601 The communication subsystem is driven by two main parameters: distance and data amount. The maximum dis-  
602 tance between Ceres and Earth in a theoretical Ceres-Sun-Earth constellation is 3.976 AU. The amount of mapping  
603 data (without source coding) is 166.66 Gbit. Surface mapping is key for choosing a suitable landing zone and there-  
604 fore the data shall be downlinked as fast as possible, using a Ka-Band System which can provide sufficient downlink  
605 speeds of up to 360 kbit/s at maximum separation. A 3 m High Gain Antenna (HGA) is used on the S/C to ensure the  
606 link and provide the needed performance.

607 The payload data system would rely on the Deep Space Network (DSN) for Ka-Band. In addition the telemetry and  
608 telecommand subsystem would use a low power, low gain X-Band emergency system which would ensure communi-  
609 cation at any attitude and would be built to ensure communication in emergency situations where power management  
610 is crucial. The expected data rate would not exceed 50 bit/s which is sufficient for emergencies in any mission phases.  
611 Communication between orbiter and lander during surface operations must also be considered. This system would  
612 work in X-Band with the available X-Band antennas of the orbiter. The orbiter and lander would have a maximum  
613 distance of 500 km. Even with a lower power system of 15 W sending power and low gain antennas, 80 kbit/s can  
614 be reached with a Quadrature Phase Shift Keying (QPSK) modulation. The gathered data from the lander would then  
615 be stored and relayed to Earth with the Ka-Band payload data system. The orbiter uses the already available X-Band  
616 radio system for this type of communication, while the lander carries a Ka-Band radio system, which provides the  
617 aforementioned data rate and sends power paired with an antenna that provides a circular gain pattern

### 618 *6.4. Data handling Subsystem*

619 The design of the On-board Data Handling (OBDH) subsystem is mainly driven by the long mission duration, the  
620 limited down-link capacity to the ground station and the power requirements on the lander. The long mission duration  
621 makes hardware with ample flight heritage favourable. Due to the limited down-link capacity to the ground station,  
622 mass memory on-board is required. European heritage, such as the LEON-FT processor, are preferred. Out of these  
623 factors, the design is mainly driven by memory requirements, leaving the processing power as secondary importance.  
624 The Next Generation On Board Computer by RUAG, which has mass memory modules available in different sizes, is  
625 suggested for the orbiter.

626 Data rates of different mission phases are taken into account to decide on the orbiter memory. The most data intensive  
627 phases are the mapping phases, where a large amount of images has to be stored before they can be down-linked.  
628 After the mapping phase, a maximum of 167 Gbits need to be stored and down-linked in the following 133 days.  
629 Therefore a NAND Flash Module - DDC with 196 Gbit is chosen. The case of storing the full series of images during  
630 the mapping is considered as a worst case scenario.

631 The Processor Board from RUAG, due to its smaller form factor, is suggested as the computing module for the  
632 lander, while a mass memory has to be added separately. The Processor Board can be optionally equipped with the  
633 RTAX 2000 FPGA, which might be of interest for the computationally expensive control algorithms for the landing  
634 procedure.

### 635 *6.5. Power Subsystem*

636 Since no feasible alternative to a solar power generator for the mission timescale and power ratings is conceiv-  
637 able, the spacecraft is powered by state-of-the-art multi-junction solar cells designed for low-intensity applications.  
638 Sample preservation issues demand short time-of-flight for the Ceres-Earth orbit, therefore the preliminary design of  
639 the size of the solar power generator is driven by the power required by the ion engines to fulfil the thrust profile for

640 the designed orbit. In this case, a class 100 kW Begin-of-Life (AM0) solar array is required. Although such a power  
641 rating represents a technological challenge, new promising solutions could be tailored for the needs of the mission  
642 due to their flexibility, modularity and scalability. As a first-approach design, the MegaFlex Solar Array technology  
643 [89] is considered, leading to a structure consisting of two circular flexible panels with a diameter of 16 m. Further  
644 iterations of the orbit design would lead to an optimized solution and would reduce the solar panels area significantly.  
645 The energy storage system for the spacecraft is expected not to pose any technological challenges. The orbiter is  
646 equipped with a battery system based on Li-Ion 18650 cell technology with a nominal capacity of 7.5 kWh, capable  
647 of powering the spacecraft during eclipse and recovery phases. The lander, on the other hand, is equipped with a  
648 redundant dual battery system (primary + secondary). The primary battery is based on LiSOCl<sub>2</sub> technology, equipped  
649 with a de-passivation circuit to remove the passivation layer formed during the cruise phase. Ground testing on a  
650 twin battery would facilitate the estimation of the capacity during the landing and scientific operation phases. The  
651 secondary battery is based on re-chargeable Li-Ion technology. It is supplied by the orbiter solar panels via umbilical  
652 line during the cruise phase. Within the 10 Earth days required to perform the scientific operations at Ceres' surface,  
653 an optimized schedule of the drilling phase with the data transmission windows leads to a minimum battery capacity  
654 of 3.8 kWh [90]. The scientific operations at Ceres, scheduled within 10 Earth days, may be subjected to significant  
655 delays due to anomaly procedures. Further iterations on the science operation schedule at Ceres surface have to be  
656 performed to account for this scenario, which can lead to an increased size of the secondary battery and to a cus-  
657 tomized solution for a lander solar generator.  
658 The ascent module is equipped with a primary battery of the same technology. In this case, to ensure the worst case  
659 autonomy of 48 hours during the ascent and docking phase, a total capacity of 1.4 kWh is required. All the batteries  
660 are equipped with thermistors and heaters to ensure proper temperature control in the optimal storage range provided  
661 by the manufacturer. The sizing has been done taking into account a subsystem margin of 20%.

## 663 6.6. Thermal Control Subsystem

664 The thermal control subsystems of the orbiter and the lander ensures the correct temperature of all subsystems dur-  
665 ing the whole mission. From the mission requirements, no separate thermal control measures have to be implemented  
666 on the samples at any point. Table 2 depicts the temperature requirements for the spacecrafts and the respective sub-  
systems, which limit the allowed temperature ranges.

Table 2: Temperature range requirements

	$T_{min}$ [°C]	Limiting subsystem	$T_{max}$ [°C]	Limiting subsystem
Orbiter	25	Xenon propellant	40	Camera and electronics
Lander	10	Hydrazine propellant	40	Camera and electronics

667 As the dominant mechanism of heat exchange between the spacecraft and its environment is thermal radiation, a com-  
668 bination of radiators including louvers, which are controlled passively by bimetal springs, multi-layer insulation, heat  
669 pipes and small polyimide heaters would be sufficient to regulate the temperature of the two spacecrafts with minimal  
670 power consumption. The proposed system can cope with the unsteady thermal environment of the spacecraft, espe-  
671 cially during the two most extreme cases of the mission: the hot first phase of the mission, during which the spacecraft  
672 experiences the greatest heat flux from the Sun, and the cold environment both orbiter and lander have to withstand  
673 in later mission phases at Ceres. Tables 3 and 4 depict the contrast of these two most extreme thermal cases for the  
674 orbiter and the lander.

Table 3: Thermal environment of the orbiter

Case definition	Sun heat flux [W/m <sup>2</sup> ]		Infrared emission [W/m <sup>2</sup> ]		Albedo [%]	Equilibrium temperature [°C]	
	Min	Max	Min	Max		Min	Max
Earth Escape	0	1414	216	258	34	-81.1	78.2
Ceres 100 km orbit	0	159.5	14.6	81.7	9	-138.9	-71.5

675

Table 4: Thermal environment of the lander

Case definition	Sun heat flux [W/m <sup>2</sup> ]	Infrared emission [W/m <sup>2</sup> ]	Conduction [W/m <sup>2</sup> ]	Surface temperature [°C]
Daytime at Ceres	159.5	144	0.4	-40
Nighttime at Ceres	0	26	1	-143

### 6.7. Navigation and Control system

Two separate navigation and control subsystems are required for the Calathus mission, one on the orbiter and on the Piazzoli lander. The navigation system of the orbiter is composed of star trackers (5 arcsec precision), sun sensors, Inertial Measurements Unit (IMU) and navigation cameras with a field of view of  $25^\circ \times 19^\circ$  and  $2592 \times 1994$  px. The Piazzoli lander carries a set of sensors to allow landing and orbital operation during ascent and on-orbit operation: star trackers - to be used in the orbital phase - IMU, navigation camera and an altimeter, to allow landing.

The control system of the orbiter is composed of reaction wheels and ACDS thrusters to allow pointing and compensate perturbations. The same sensors are carried by the lander in order to ensure the correct orientation of the instrument suite during descent, landing and ascent.

The main driving factor for determining the control system for the orbiter is the orientation velocity required to have pointing during low altitude mapping of the cerean surface, as the camera must be pointed towards the crater: this implies an angular velocity of about 0.1 deg/s provided by the reaction wheels and a pointing precision of 50 arcsec. A momentum dumping of about 2 N given by the thrusters is required after wheel saturation and it is crucial to design the thrusters cluster for this and for housekeeping manoeuvres.

The main driving requirements for designing the lander control subsystem is to ensure the correct orientation of the lander during the descent trajectory so the instrument platform is correctly oriented. The reaction wheels are crucial to provide the required angular velocity of 0.04 deg/s. This requirement has been deduced from the guidance trajectory introduced in Section 4.4. Moreover, in order to brake the spacecraft during landing, the thrusters are designed to provide force of 0.25 N which is consistent with the proposed trajectory. The navigation suite has been designed to provide a precision of about 75 arcsec by combining laser altimeter, navigation camera and IMU.

Both the lander and the orbiter are equipped with a cluster of 12 thrusters which allows redundant control in all translational and rotational directions. Reaction wheels are redundant to avoid system failure (for example as occurred during the Hayabusa mission [91]). Similarly to previous mission to small bodies [91, 92, 93, 94, 95], the critical navigation sensors, such as navigation cameras, star trackers and IMUs, are redundant to minimise mission failure. A set of 16 Sun-sensors are used as in previous missions. The altimeter of the lander is similar to the laser-range finder used by the Hayabusa2 probe as it is less power demanding than the flash LIDAR carried on OSIRIS-REx [96].

### 6.8. Landing System

The mission is expected to use active landing with obstacle avoidance software. This subsystem is required to ensure low velocity impact and safe landing. A critical subsystem is the landing gear to damp the residual velocity and ensure structural integrity. This is a crucial issue that can take advantages from the heritage of previous lunar, martian and small body missions. Nevertheless, it is important to notice that Ceres has its own peculiar environment to be considered: neither an extreme low-gravity body, which implies problem in bouncing and anchoring to the surface, nor a dwarf planet with atmosphere, which implies aerodynamical forces during descent. The absence of these two problems implies that landing on Ceres is expected to be easier to accomplish. Further analysis should be conducted to identify the subsystem requirements and the subsystem optimal design. Moreover, as the mapping of the landing site would have a resolution of 0.6 m/px, an active hazardous detection and avoidance system is necessary to fulfil mission requirements (see Section 3). This system ensures that the lander can dodge boulders and other obstacles in order to land at a hazardous-free spot close to the nominal landing site. This technology has not been used on other celestial bodies. A first try of hazardous detection and avoidance will be implemented in the Chinese Mars lander set to launch in 2020 [97] and, as a consequence, further technological development is required. The nominal algorithm would be based on cameras and LIDAR data fusion for safe and pinpoint landing [98].

### 6.9. Sample Canister Catching Subsystem

A crucial operation for the Calathus mission is the sample canister catching. This implies that a careful design must be put in place in order to ensure the fulfilment of mission goals. The main heritage of this design is Mars

720 Sample Return [68] for the canister catching and identification during flight. The cooperative rendez-vous design is  
 721 based on the experience obtained from the ATV and the design of vision-based navigation solution for cooperative  
 722 rendez-vous in the Earth environment [99, 100, 101].  
 723 The first phase is the cooperative rendez-vous between the two spacecraft. The control systems of the orbiter and the  
 724 ascending module are used to keep the relative position and orientation correct while the relative navigation is ensured  
 725 by a continuous radio communication, which is obtained from the LGA carried from both spacecraft. The use of the  
 726 LGA ensures that even when the two spacecraft are distant, relative localization and position can be performed by  
 727 knowing the position and velocity in the cerean reference frame. Thanks to this information the two spacecraft can  
 728 operate and reduce their spacial separation. Then the close approach between the two spacecraft starts. Vision-based  
 729 algorithms, such as spacecraft model tracking [99, 100], ensures that the orbiter correctly localises and orients itself  
 730 with respect to the ascending module. This phase starts when the two spacecraft have a spatial separation of about 150  
 731 m that allows the main spacecraft to identify shape details in the image of the ascending module to be matched with  
 732 the model during tracking. When the first phase is completed, the canister is ejected from the ascending module. This  
 733 phase starts when the spatial separation between the two spacecraft is 25 m. In order to correctly localise the canister,  
 734 it is covered in LED lights and solar cells (which ensure high reflectively with respect to incident laser beams),  
 735 which can be tracked from the navigation camera. Laser pulses are emitted from the LIDAR on the orbiter, which ensures  
 736 accurate localisation of the canister at close distance. The tracking is supported by the same vision-based navigation  
 737 with model tracking as the previous phase. The LED tracking technique is similar to the technology that has been  
 738 used for the touchdown operation of the Hayabusa2 spacecraft at Ryugu [102]. The relative orientation and position  
 739 is controlled accordingly to ensure that the sample canister enters in the capture cone, as depicted in Figure 13b. Once  
 the canister is inside of the main spacecraft, a sliding mechanism pulls the sample canister into the reentry capsule.

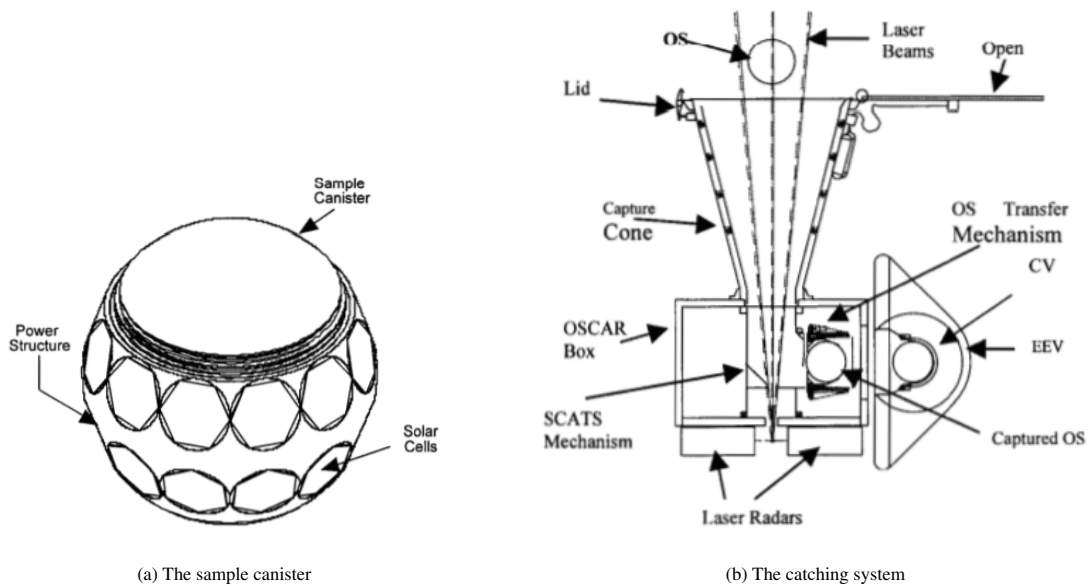


Figure 13: The Mars Sample Return heritage (see [68])

740

### 741 6.10. Re-entry capsule

742 Since a sample return mission to Ceres falls under class V restricted regulations, the re-entry capsule has to follow  
 743 a very tight design guideline. The sample is under no circumstances allowed to contaminate Earth when returning  
 744 to Earth. Therefore a crushable structure is suggested [103] which would take the whole load of the impact. A  
 745 parachute is not considered since it could for instance rupture and then a harder than expected impact could result in  
 746 contamination. A landing in water is not allowed although the transport container would be water tight. Only three  
 747 possible landing zones exist on Earth: the great salt desert in Utah (USA), the Kazakh desert in Kazakhstan, and  
 748 the Australian Woomera desert. The landing site would be selected when the return trajectory is well known. The

749 nominal re-entry would be in the Woomera desert as the Australian government has experience with the recovery of  
 750 reentry capsule as performed during the Hayabusa mission. The design of the reentry capsule is taken as heritage from  
 751 previous missions concept, such as Mars Sample Return’s capsule [104].

## 752 **7. Mission budget and risks**

### 753 *7.1. Mass budget*

754 The preliminary wet mass budget estimate for Calathus is of 5880 kg (including 20% system margin and the  
 755 launch adapter) as presented in Table 5. Considering the Ariane 64 launch capacity of 7667 kg, a launch margin  
 756 of about 1520 kg is available, which makes is possible to embark a small spacecraft, possibly a secondary science  
 757 payload, together with Calathus. The fuel comprises the most critical part of the mass budget which is 3373 kg, which  
 is essential to achieve the itinerary to Ceres.

Table 5: Launcher and spacecraft current best mass budgets estimates.

Mass Budget	Mass [kg]
GNC	46
Communications	103
Data Handling	20
Instruments	53
Mechanisms	97
Propulsion	373
Power	758
Structure	379
Thermal Control	83
Harness	94
Spacecraft Dry Mass (including 20% system margin)	2407
Mass consumables	3373
Wet mass	5780
Launcher adapter	100
Total wet mass + Launcher adapter	5880
Ariane 64 launch capacity	7400
Margin	1520

758

### 759 *7.2. Power budget*

760 For the Calathus mission, the main power consumption modes are highlighted in Tables 6 and 7. The power  
 761 consumption of each mission phase is reported for each subsystem, considering worst case operations and a 20%  
 762 subsystem margin. The power required by the ion engines during the inbound and outbound trajectories is by far the  
 763 main driver for the solar panel design. For this reason, the propulsion power has been intentionally omitted in this  
 764 section.

### 765 *7.3. Programmatics*

766 Within ESA’s Cosmic Vision framework, the Calathus mission would be classified as an L-class mission. It is  
 767 expected to produce answers to some fundamental questions about the evolution of asteroids in the Solar System,  
 768 astrobiology, and the delivery of volatiles and organics to Earth. Although estimating cost is challenging, it will be a  
 769 programmatic challenge to ensure the budget for the mission does not exceed the cost cap of 1000 ~ M€ for L-class  
 770 missions. This is in part due to the multiple elements of this mission, and the large number of technologies involve.  
 771 Additionally, planetary protection technologies are a large driver of cost, as engineering decisions have been made  
 772 which, whilst favourable to reduce planetary protection concerns, may be more expensive. An example of this would

Table 6: Power modes for the Orbiter and Orbiter subsystems: Attitude and Orbit Control (AOCS), Communication (COMS), Data Handling (DH), Payload Instrumentation (PAY), Mechanism (MEC), Power distribution (POW) and Thermal Control (THER).

Orbiter Mode	AOCS [W]	COMS [W]	DH [W]	PAY [W]	MEC [W]	POW [W]	THER [W]	TOTAL [W]
Mapping	36	0	23	45	12	18	22	157
Comm	36	503	23	0	72	18	22	675
Relay	36	523	23	0	72	18	22	695
Sample Catch	36	0	23	0	42	18	22	142
Eclipse	36	0	23	18	12	18	22	130
Safe	36	80	23	0	12	18	22	192

Table 7: Power modes for the Lander and Lander subsystems: Attitude and Orbit Control (AOCS), Communication (COMS), Data Handling (DH), Payload Instrumentation (PAY), Mechanism (MEC), Power distribution (POW), Thermal Control (THER) and Propulsion (PROP).

Lander Mode	AOCS [W]	COMS [W]	DH [W]	INS [W]	MEC [W]	POW [W]	TC [W]	PROP [w]	TOTAL [W]
Descent	37	0	6	8	0	3	5	58	118
SciOps	0	0	7	2	70	3	5	0	87
Idle	0	0	1	0	0	3	5	0	9
Ascent	37	0	7	0	0	3	5	58	110
In Situ	0	0	7	10	0	3	5	0	25
Transmission	0	55	7	0	0	3	0	0	65

773 be the re-entry capsule for which special attention will have to be applied in order not to contaminate the Earth after  
774 landing.

775 Comparisons can be made to similar missions, for example OSIRIS-REx cost \$1.16 billion, with \$588.5 million for  
776 spacecraft development, \$183.5 million for the launch vehicle and \$283 million for 9 years of operations [105]. How-  
777 ever, Calathus does have more elements including separate orbiter and lander segments. In fact, current estimations  
778 calculate the most expensive aspect is the orbiter segment. This is because the cost estimate is calculated by multiply-  
779 ing correction factors (depending on complexity) by the dry mass. The costs lowers when payload or techniques are  
780 already tested and used. A deeper analysis of the mission’s subsystem could help refining the cost estimation.

781 When considering the risks presented by this mission design, the low TRL of enabling technology must be considered.  
782 The success of the mission depends on the presence of some technologies with current TRL levels of only 3 (e.g. the  
783 sampling mechanism) and 4 (e.g. active descent) in order to achieve the scientific objectives. However, with a launch  
784 date in 2031, at the time of writing there is still 11 years of development time for these low TRL technologies, and  
785 as such the risk here is acceptable. For example, the sample capsule ascent and docking with the main spacecraft  
786 mechanism is being developed as part of Mars Sample Return, so it is anticipate that despite its low TRL, this would  
787 be adequately developed by the launch window [68].

788 Another concern is the issue of Planetary Protection. Due to the class V restricted nature of samples returned from  
789 Ceres, an additional risk is the terrestrial contamination both of the samples collected and back contamination of Earth  
790 with the returned samples. To tackle the former, the lander ascent/descent manoeuvres would be controlled using a  
791 monopropellant hydrazine thruster to reduce the amount of contamination of the surface of Ceres, and the collected  
792 samples would be stored in the sealed reentry capsule until it reaches the curation facility on Earth. For protection of  
793 Earth, the re-entry capsule would not use a parachute, and would have a crushable structure to minimise chance of the  
794 capsule breaking upon impact.

## 795 8. Conclusion

796 In this paper, the case for a return to Ceres and for a sample of this dwarf planet to be returned to Earth is outlined.  
797 The Calathus mission is a concept that aims to bring 4 samples of 4 cm<sup>3</sup> of the bright carbonate material from Ceres’  
798 Occator Crater by 2050. This is to understand the astrobiological potential of relict ocean-bearing worlds, and also the  
799 origins and dynamics of the Solar System’s configuration — and in doing so, to understand how water was delivered  
800 to Earth, along with the organic molecules that could through time evolve into life.

801 A sample return mission to Ceres is the ideal next step in ESA’s plan to understand the Solar System, and in doing



Table 8: Estimation of the mission’s cost

	Cost (Million €)
Orbiter	2.7
Lander	0.72
Development and Manufacturing	3335
Ground segment	148
Launcher	132
Grand total	~ 3600

so to ultimately understand life’s origins. The technology developed and trialled during Calathus would enhance the likelihood of the actualisation of future missions high in ESA’s priority for outer Solar System exploration, including sample return from the more-technologically demanding Jovian and Saturnian moons. In essence, however, Calathus represents the exploration of a fascinating world within its own right. Ceres is a world rich in water, organics, and has a geologic history open and prime for in-situ exploration. Calathus could become humans’ eyes and hands on the ground before returning to Earth — the first mission to ever do so on a planet-sized body. The Calathus mission is therefore Europe’s means of leading humanity’s next flagship, historic space mission, one in the vein of Rosetta-Philae and Cassini’s Huygens probe: a means of pioneering the next step in the evolution of spaceflight.

## 9. Acknowledgements

The authors acknowledge ESA and the FFG (the Austrian Research Promotion Agency) for the funding to attend the Post Alpbach Summer School Event 2018. This study benefited from the work of 40 other students during the Summer School Alpbach 2018 on "Sample Return from small solar system bodies". The authors also would like to thank all the tutors and organisers of the summer school for their support. The authors thank Marcus Hallmann for the PaGMO implementation of the outbound optimization.

## 10. Authors contribution

The author list is divided in three different lists. Oriane Gassot and Paolo Panicucci managed the coordination among the other authors to make this paper possible. The name appearing in the first alphabetical list, from Giacomo Acciarini to Clemens Riegler, have worked on the paper redaction and mission design after the Post Alpbach Summer School Event 2018. The other authors have contributed to the design during the Alpbach Summer School and the Post Alpbach Summer School Event 2018.

## References

### References

- [1] Amanda R. Hendrix, Terry A. Hurford, Laura M. Barge, Michael T. Bland, Jeff S. Bowman, William Brinckerhoff, Bonnie J. Buratti, Morgan L. Cable, Julie Castillo-Rogez, Geoffrey C. Collins, Serina Diniega, Christopher R. German, Alexander G. Hayes, Tori Hoehler, Sona Hosseini, Carly J.A. Howett, Alfred S. McEwen, Catherine D. Neish, Marc Neveu, Tom A. Nordheim, G. Wesley Patterson, D. Alex Patthoff, Cynthia Phillips, Alyssa Rhoden, Britney E. Schmidt, Kelsi N. Singer, Jason M. Soderblom, and Steven D. Vance. The nasa roadmap to ocean worlds. *Astrobiology*, 19(1):1–27, 2019. doi: 10.1089/ast.2018.1955.
- [2] Michael H Carr, Michael JS Belton, Clark R Chapman, Merton E Davies, Paul Geissler, Richard Greenberg, Alfred S McEwen, Bruce R Tufts, Ronald Greeley, Robert Sullivan, et al. Evidence for a subsurface ocean on europa. *Nature*, 391(6665):363, 1998.
- [3] Carolyn C Porco, P Helfenstein, PC Thomas, AP Ingersoll, J Wisdom, R West, G Neukum, T Denk, R Wagner, Th Roatsch, et al. Cassini observes the active south pole of enceladus. *science*, 311(5766):1393–1401, 2006.
- [4] Julie C Castillo-Rogez, Marc Neveu, Jennifer EC Scully, Christopher H House, Lynnae C Quick, Alexis Bouquet, Kelly Miller, Michael Bland, Maria Cristina De Sanctis, Anton Ermakov, Amanda R. Hendrix, Thomas H. Prettyman, Carol A. Raymond, Christopher T. Russell, Brent E. Sherwood, and Edward Young. Ceres: astrobiological target and possible ocean world. *Astrobiology*, 20(2):269–291, 2020.
- [5] Maria Cristina De Sanctis, Giuseppe Mitri, Julie Castillo-Rogez, Christopher H House, Simome Marchi, Carol A Raymond, and Yasuhito Sekine. Relict ocean worlds: Ceres. *SPACE SCIENCE REVIEWS*, 216(4), 2020.

- 838 [6] K. K. Khurana, V. Angelopoulos, M. G. Kivelson, and C. T. Russell. Characterizing Europa's Subsurface Water Ocean from Future  
839 Electromagnetic Induction Studies. In *Workshop on the Habitability of Icy Worlds*, volume 1774, page 4081, February 2014.
- 840 [7] Steve Vance, Jelte Harnmeijer, Jun Kimura, Hauke Hussmann, Brian DeMartín, and J Michael Brown. Hydrothermal systems in small ocean  
841 planets. *Astrobiology*, 7(6):987–1005, 2007.
- 842 [8] Low temperature condensation from the solar nebula. *Icarus*, 16(2):241 – 252, 1972. ISSN 0019-1035. doi: [https://doi.org/10.1016/0019-1035\(72\)90071-1](https://doi.org/10.1016/0019-1035(72)90071-1).
- 843 [9] K. L. Mitchell and R. M. C. Lopes. Cryovolcanism on Titan. In *Cryovolcanism in the Solar System Workshop*, volume 2045, page 2037,  
844 June 2018.
- 845 [10] TB a McCord, GB Hansen, RN Clark, PD Martin, CA Hibbitts, FP Fanale, JC Granahan, M Segura, DL Matson, TV Johnson, et al. Non-  
846 water-ice constituents in the surface material of the icy galilean satellites from the galileo near-infrared mapping spectrometer investigation.  
847 *Journal of Geophysical Research: Planets*, 103(E4):8603–8626, 1998.
- 848 [11] Frank Postberg, Nozair Khawaja, Bernd Abel, Gael Choblet, Christopher R Glein, Murthy S Gudipati, Bryana L Henderson, Hsiang-Wen  
849 Hsu, Sascha Kempf, Fabian Klenner, et al. Macromolecular organic compounds from the depths of enceladus. *Nature*, 558(7711):564,  
850 2018.
- 851 [12] Gene D McDonald, W Reid Thompson, Michael Heinrich, Bishun N Khare, and Carl Sagan. Chemical investigation of titan and triton  
852 tholins. *Icarus*, 108(1):137–145, 1994.
- 853 [13] MC De Sanctis, E Ammannito, HY McSween, A Raponi, S Marchi, F Capaccioni, MT Capria, FG Carrozzo, M Ciarniello, S Fonte, et al.  
854 Localized aliphatic organic material on the surface of ceres. *Science*, 355(6326):719–722, 2017.
- 855 [14] WM Grundy, RP Binzel, BJ Buratti, JC Cook, DP Cruikshank, CM Dalle Ore, AM Earle, K Ennico, CJA Howett, AW Lunsford, et al.  
856 Surface compositions across pluto and charon. *Science*, 351(6279):aad9189, 2016.
- 857 [15] Marc Neveu and Steven J. Desch. Geochemistry, thermal evolution, and cryovolcanism on ceres with a muddy  
858 ice mantle. *Geophysical Research Letters*, 42(23):10,197–10,206, 2015. doi: 10.1002/2015GL066375. URL  
859 <https://agupubs.onlinelibrary.wiley.com/doi/abs/10.1002/2015GL066375>.
- 860 [16] Paul H. Warren. Stable-isotopic anomalies and the accretionary assemblage of the Earth and Mars: A subordinate role for carbonaceous  
861 chondrites. *Earth and Planetary Science Letters*, 311(1):93–100, November 2011. doi: 10.1016/j.epsl.2011.08.047.
- 862 [17] MC De Sanctis, E Ammannito, A Raponi, S Marchi, TB McCord, HY McSween, F Capaccioni, MT Capria, FG Carrozzo, M Ciarniello,  
863 et al. Ammoniated phyllosilicates with a likely outer solar system origin on (1) ceres. *Nature*, 528(7581):241, 2015.
- 864 [18] E Ammannito, MC DeSanctis, M Ciarniello, A Frigeri, FG Carrozzo, J-Ph Combe, BL Ehlmann, S Marchi, HY McSween, A Raponi, et al.  
865 Distribution of phyllosilicates on the surface of ceres. *Science*, 353(6303):aaf4279, 2016.
- 866 [19] T. H. Prettyman, N. Yamashita, M. J. Toplis, H. Y. McSween, N. Schörghofer, S. Marchi, W. C. Feldman, J. Castillo-Rogez, O. Forni, D. J.  
867 Lawrence, E. Ammannito, B. L. Ehlmann, H. G. Sizemore, S. P. Joy, C. A. Polansky, M. D. Rayman, C. A. Raymond, and C. T. Russell.  
868 Extensive water ice within ceres' aqueously altered regolith: Evidence from nuclear spectroscopy. *Science*, 355(6320):55–59, 2017. ISSN  
869 0036-8075. doi: 10.1126/science.aah6765. URL <https://science.sciencemag.org/content/355/6320/55>.
- 870 [20] COSPAR Panel on Planetary Protection. Cospas policy on planetary protection. *Space Research Today*, (208):10–22, 2020.
- 871 [21] Giacomo Acciarini, Helena Bates, Nini Berge, Manel Caballero, Pamela Cambianica, Maciej Dziewiecki, Zelia Dionnet, Felix Enengl,  
872 Oriane Gassot, Selina-Barbara Gerig, Felix Hessinger, Nikolaus Huber, Richard Hynek, Bartosz Kędziora, Lucy Kissick, Adam Kiss,  
873 MAurice Martin, Javier Navarro Montilla, Moritz Novak, Paolo Panicucci, Carmine Pellegrino, Angèle Pontoni, Tania Ribeiro, and Riegler  
874 Clemens. Sample return from a relic ocean world: The calathus mission to occator crater, ceres. In *Proceedings of the 16th International  
875 Planetary Probe Workshop*, 2019.
- 876 [22] Giacomo Acciarini, Helena Bates, Nini Berge, Manel Caballero, Pamela Cambianica, Maciej Dziewiecki, Zelia Dionnet, Felix Enengl,  
877 Oriane Gassot, Selina-Barbara Gerig, Felix Hessinger, Nikolaus Huber, Richard Hynek, Bartosz Kędziora, Lucy Kissick, Adam Kiss,  
878 MAurice Martin, Javier Navarro Montilla, Moritz Novak, Paolo Panicucci, Carmine Pellegrino, Angèle Pontoni, Tania Ribeiro, and Riegler  
879 Clemens. The calathus mission concept to occator crater at ceres: Science, operations and systems design. In *Proceedings of the Planetary  
880 Exploration - Horizon 2061*, 2019.
- 881 [23] EV Pitjeva and NP Pitjev. Masses of asteroids and total mass of the main asteroid belt. *Proceedings of the International Astronomical  
882 Union*, 10(S318):212–217, 2015.
- 883 [24] PC Thomas, J Wm Parker, LA McFadden, Cc T Russell, SA Stern, MV Sykes, and EF Young. Differentiation of the asteroid ceres as  
884 revealed by its shape. *Nature*, 437(7056):224, 2005.
- 885 [25] Thomas B McCord, Lucy A McFadden, Christopher T Russell, Christophe Sotin, and Peter C Thomas. Ceres, vesta, and pallas: protoplanets,  
886 not asteroids. *Eos, Transactions American Geophysical Union*, 87(10):105–109, 2006.
- 887 [26] Christopher Russell and Carol Raymond. *The Dawn Mission to Minor Planets 4 Vesta and 1 Ceres*. Springer Science & Business Media,  
888 2012.
- 889 [27] AS Konopliv, RS Park, AT Vaughan, BG Bills, SW Asmar, AI Ermakov, N Rambaux, CA Raymond, JC Castillo-Rogez, CT Russell, et al.  
890 The ceres gravity field, spin pole, rotation period and orbit from the dawn radiometric tracking and optical data. *Icarus*, 299:411–429, 2018.
- 891 [28] Thomas B McCord and Francesca Zambon. The surface composition of ceres from the dawn mission. *Icarus*, 318:2–13, 2019.
- 892 [29] Paul O Hayne and Oded Aharonson. Thermal stability of ice on ceres with rough topography. *Journal of Geophysical Research: Planets*,  
893 120(9):1567–1584, 2015.
- 894 [30] Jian-Yang Li, Vishnu Reddy, Andreas Nathues, Lucille Le Corre, Matthew RM Izawa, Edward A Cloutis, Mark V Sykes, Uri Carsenty,  
895 Julie C Castillo-Rogez, Martin Hoffmann, et al. Surface albedo and spectral variability of ceres. *The Astrophysical Journal Letters*, 817(2):  
896 L22, 2016.
- 897 [31] Clark R Chapman and John W Salisbury. Comparisons of meteorite and asteroid spectral reflectivities. *Icarus*, 19(4):507–522, 1973.
- 898 [32] Thomas B McCord and Michael J Gaffey. Asteroids: Surface composition from reflection spectroscopy. *Science*, 186(4161):352–355, 1974.
- 899 [33] Harry Y McSween Jr, Joshua P Emery, Andrew S Rivkin, Michael J Toplis, Julie C. Castillo-Rogez, Thomas H Prettyman, M Cristina  
900 De Sanctis, Carle M Pieters, Carol A Raymond, and Christopher T Russell. Carbonaceous chondrites as analogs for the composition and  
901 alteration of ceres. *Meteoritics & Planetary Science*, 53(9):1793–1804, 2018.
- 902

- 903 [34] DL Buczkowski, BE Schmidt, DA Williams, SC Mest, JEC Scully, AI Ermakov, F Preusker, P Schenk, KA Otto, H Hiesinger, et al. The  
904 geomorphology of ceres. *Science*, 353(6303):aaf4332, 2016.
- 905 [35] O Ruesch, T Platz, P Schenk, LA McFadden, JC Castillo-Rogez, LC Quick, Shane Byrne, F Preusker, DP O'Brien, N Schmedemann, et al.  
906 Cryovolcanism on ceres. *Science*, 353(6303):aaf4286, 2016.
- 907 [36] F Zambon, A Raponi, F Tosi, MC De Sanctis, LA McFadden, FG Carrozzo, A Longobardo, M Ciarniello, K Krohn, K Stephan, et al.  
908 Spectral analysis of ahuna mons from dawn mission's visible-infrared spectrometer. *Geophysical Research Letters*, 44(1):97–104, 2017.
- 909 [37] Emily Lakdawalla. Recent cryovolcanism in virgil fossae on pluto. *LPSC*, 2015.
- 910 [38] A Raponi, MC De Sanctis, FG Carrozzo, M Ciarniello, JC Castillo-Rogez, E Ammannito, A Frigeri, A Longobardo, E Palomba, F Tosi,  
911 et al. Mineralogy of occator crater on ceres and insight into its evolution from the properties of carbonates, phyllosilicates, and chlorides.  
912 *Icarus*, 320:83–96, 2019.
- 913 [39] MC De Sanctis, A Raponi, E Ammannito, M Ciarniello, MJ Toplis, HY McSween, JC Castillo-Rogez, BL Ehlmann, FG Carrozzo, S Marchi,  
914 et al. Bright carbonate deposits as evidence of aqueous alteration on (1) ceres. *Nature*, 536(7614):54, 2016.
- 915 [40] Filippo Giacomo Carrozzo, Maria Cristina De Sanctis, Andrea Raponi, Eleonora Ammannito, Julie Castillo-Rogez, Bethany L Ehlmann,  
916 Simone Marchi, Nathaniel Stein, Mauro Ciarniello, Federico Tosi, et al. Nature, formation, and distribution of carbonates on ceres. *Science*  
917 *advances*, 4(3):e1701645, 2018.
- 918 [41] Occator crater in color at highest spatial resolution. *Icarus*, 320:24 – 38, 2019. ISSN 0019-1035. doi:  
919 <https://doi.org/10.1016/j.icarus.2017.12.021>. Occator Crater on Ceres.
- 920 [42] A Nathues, T Platz, G Thangjam, M Hoffmann, K Mengel, EA Cloutis, L Le Corre, V Reddy, J Kallisch, and DA Crown. Evolution of  
921 occator crater on (1) ceres. *The Astronomical Journal*, 153(3):112, 2017.
- 922 [43] O Ruesch, LC Quick, ME Landis, MM Sori, O Čadek, P Brož, KA Otto, MT Bland, Shane Byrne, JC Castillo-Rogez, et al. Bright carbonate  
923 surfaces on ceres as remnants of salt-rich water fountains. *Icarus*, 320:39–48, 2019.
- 924 [44] Thomas B McCord and Julie C Castillo-Rogez. Ceres' evolution before and after dawn: Where are we now? In *AAS/Division for Planetary*  
925 *Sciences Meeting Abstracts# 48*, volume 48, 2016.
- 926 [45] Preferential formation of sodium salts from frozen sodium-ammonium-chloride-carbonate brines – implications for ceres' bright spots.  
927 *Planetary and Space Science*, 141:73 – 77, 2017. ISSN 0032-0633. doi: <https://doi.org/10.1016/j.pss.2017.04.014>.
- 928 [46] Harry Y McSween, David W Mittlefehldt, Andrew W Beck, Rhiannon G Mayne, and Timothy J McCoy. Hed meteorites and their relation-  
929 ship to the geology of vesta and the dawn mission. In *The Dawn Mission to Minor Planets 4 Vesta and 1 Ceres*, pages 141–174. Springer,  
930 2010.
- 931 [47] CM O'D Alexander, R Bowden, ML Fogel, KT Howard, CDK Herd, and LR Nittler. The provenances of asteroids, and their contributions  
932 to the volatile inventories of the terrestrial planets. *Science*, 337(6095):721–723, 2012.
- 933 [48] Bernard Marty, Guillaume Avice, Yuji Sano, Kathrin Altwegg, Hans Balsiger, Myrtha Hässig, Alessandro Morbidelli, Olivier Mousis, and  
934 Martin Rubin. Origins of volatile elements (h, c, n, noble gases) on earth and mars in light of recent results from the rosetta cometary  
935 mission. *Earth and Planetary Science Letters*, 441:91–102, 2016.
- 936 [49] MARIA CRISTINA De Sanctis, E Ammannito, Andrea Raponi, S Marchi, TB McCord, HY McSween, F Capaccioni, MT Capria, FIL-  
937 IPPO GIACOMO Carrozzo, Mauro Ciarniello, et al. Ammoniated phyllosilicates with a likely outer solar system origin on (1) ceres. *Nature*,  
938 528(7581):241–244, 2015.
- 939 [50] Kevin J Walsh, Alessandro Morbidelli, Sean N Raymond, DP O'brien, and AM Mandell. Populating the asteroid belt from two parent  
940 source regions due to the migration of giant planets—"the grand tack". *Meteoritics & Planetary Science*, 47(12):1941–1947, 2012.
- 941 [51] Lynnae C Quick, Debra L Buczkowski, Ottaviano Ruesch, Jennifer EC Scully, Julie Castillo-Rogez, Carol A Raymond, Paul M Schenk,  
942 Hanna G Sizemore, and Mark V Sykes. A possible brine reservoir beneath occator crater: Thermal and compositional evolution and  
943 formation of the cerealia dome and vinalia faculae. *Icarus*, 320:119–135, 2019.
- 944 [52] J Hunter Waite Jr, WS Lewis, BA Magee, JI Lunine, WB McKinnon, CR Glein, O Mousis, DT Young, T Brockwell, J Westlake, et al.  
945 Liquid water on enceladus from observations of ammonia and 40 ar in the plume. *Nature*, 460(7254):487, 2009.
- 946 [53] Olivier Grasset, MK Dougherty, A Coustenis, EJ Bunce, C Erd, D Titov, M Blanc, A Coates, P Drossart, LN Fletcher, et al. Jupiter icy  
947 moons explorer (juice): An esa mission to orbit ganymede and to characterise the jupiter system. *Planetary and Space Science*, 78:1–21,  
948 2013.
- 949 [54] Jorge Vago, Bruno Gardini, Gerhard Kminek, Pietro Baglioni, Giacinto Gianfiglio, Andrea Santovincenzo, Silvia Bayon, and Michel van  
950 Winnendael. Exomars-searching for life on the red planet. *ESA bulletin*, 126:16–23, 2006.
- 951 [55] Karl-Heinz Glassmeier, Hermann Boehnhardt, Detlef Koschny, Ekkehard Kührt, and Ingo Richter. The rosetta mission: flying towards the  
952 origin of the solar system. *Space Science Reviews*, 128(1-4):1–21, 2007.
- 953 [56] WB Banerdt, S Smrekar, P Lognonné, T Spohn, SW Asmar, D Banfield, L Boschi, U Christensen, V Dehant, W Folkner, et al. Insight: a  
954 discovery mission to explore the interior of mars. In *Lunar and planetary science conference*, volume 44, page 1915, 2013.
- 955 [57] Igor Mitrofanov, Vladimir Dolgoplov, Viktor Khartov, Alexandr Lukjanchikov, Vlad Tret'yakov, and Lev Zelenyi. " luna-glob" and"  
956 luna-resurs": science goals, payload and status. In *EGU General Assembly Conference Abstracts*, volume 16, 2014.
- 957 [58] Karen Meech and Sean N Raymond. Origin of earth's water: Sources and constraints. *Planetary Astrobiology*, page 325, 2020.
- 958 [59] S Marchi, A Raponi, TH Prettyman, MC De Sanctis, J Castillo-Rogez, CA Raymond, E Ammannito, T Bowling, M Ciarniello, H Kaplan,  
959 E. Palomba, C. T. Russell, V. Vinogradoff, and N. Yamashita. An aqueously altered carbon-rich ceres. *Nature Astronomy*, 3(2):140–145,  
960 2019.
- 961 [60] Hans Peter de Koning, Sam Gerené, Ivo Ferreira, Andrew Pickering, Friederike Beyer, and Johan Vennekens. Open concurrent design  
962 tool—esa community open source ready to go. In *6th International Conference on Systems and Concurrent Engineering for Space Applica-*  
963 *tions, Stuttgart*, 2014.
- 964 [61] Carle M Pieters and Sarah K Noble. Space weathering on airless bodies. *Journal of Geophysical Research: Planets*, 121(10):1865–1884,  
965 2016.
- 966 [62] JP Dworkin, LA Adelman, T Ajluni, AV Andronikov, JC Aponte, AE Bartels, E Beshore, EB Bierhaus, JR Brucato, BH Bryan, et al.  
967 Osiris-rex contamination control strategy and implementation. *Space science reviews*, 214(1):19, 2018.

- 968 [63] Francesco Biscani and Dario Izzo. A parallel global multiobjective framework for optimization: pagmo. *Journal of Open Source Software*,  
969 5(53):2338, 2020.
- 970 [64] Francesco Biscani, Dario Izzo, and Marcus Mörtens. esa/pagmo2: pagmo 2.7. Technical report, April 2018.
- 971 [65] Anastassios E Petropoulos and James M Longuski. Shape-based algorithm for the automated design of low-thrust, gravity assist trajectories.  
972 *Journal of Spacecraft and Rockets*, 41(5):787–796, 2004.
- 973 [66] Dario Izzo. Lambert’s problem for exponential sinusoids. *Journal of guidance, control, and dynamics*, 29(5):1242–1245, 2006.
- 974 [67] M Vasile, O Schütze, O Junge, G Radice, M Dellnitz, and D Izzo. Spiral trajectories in global optimisation of interplanetary and orbital  
975 transfers. *Ariadna Study Report AO4919*, 5:4106, 2006.
- 976 [68] H Price, K Cramer, S Doudrick, W Lee, J Matijevic, S Weinstein, T Lam-Trong, O Marsal, and R Mitcheltree. Mars sample return spacecraft  
977 systems architecture. In *2000 IEEE Aerospace Conference. Proceedings (Cat. No. 00TH8484)*, volume 7, pages 357–375. IEEE, 2000.
- 978 [69] Julie Castillo-Rogez and John Brophy. Planetary science decadal survey : Ceres: exploration of ceres’s habitability. Technical report,  
979 NASA, 2020.
- 980 [70] NASA. Planetary protection provisions for robotic extraterrestrial missions, 2005.
- 981 [71] Aurore Hutzler, Ludovic Ferrière, Allan Bennett, JR Brucato, Vincianne Debaille, Luigi Folco, Andrea Longobardo, Andrea Meneghin,  
982 Ernesto Palomba, Thomas Pottage, et al. Euro-cares sample curation facility: Preliminary design. In *79th Annual Meeting of the Meteoritical  
983 Society*, volume 1921, 2016.
- 984 [72] Horst Uwe Keller, Cesare Barbieri, Philippe Lamy, Hans Rickman, Rafael Rodrigo, K-P Wenzel, Holger Sierks, Michael F A’Hearn,  
985 Francesco Angrilli, M Angulo, et al. Osiris—the scientific camera system onboard rosetta. *Space Science Reviews*, 128(1-4):433–506, 2007.
- 986 [73] RW Gaskell, OS Barnouin-Jha, Daniel J Scheeres, AS Konopliv, T Mukai, S Abe, J Saito, M Ishiguro, T Kubota, T Hashimoto, et al.  
987 Characterizing and navigating small bodies with imaging data. *Meteoritics & Planetary Science*, 43(6):1049–1061, 2008.
- 988 [74] RW Gaskell. Automated landmark identification for spacecraft navigation. 2001.
- 989 [75] Tatsuaki Okada, Tetsuya Fukuhara, Satoshi Tanaka, Makoto Taguchi, Takeshi Imamura, Takehiko Arai, Hiroki Senshu, Yoshiko Ogawa, Hi-  
990 rohide Demura, Kohei Kitazato, Ryosuke Nakamura, Toru Kouyama, Tomohiko Sekiguchi, Sunao Hasegawa, Tsuneo Matsunaga, Takehiko  
991 Wada, Jun Takita, Naoya Sakatani, Yamato Horikawa, Ken Endo, Jörn Helbert, Thomas G. Müller, and Axel Hagermann. Thermal infrared  
992 imaging experiments of c-type asteroid 162173 ryugu on hayabusa2. *Space Science Reviews*, 208(1):255–286, Jul 2017. ISSN 1572-9672.  
993 doi: 10.1007/s11214-016-0286-8.
- 994 [76] Roberto Seu, Roger J Phillips, Daniela Biccari, Roberto Orosei, Arturo Masdea, Giovanni Picardi, Ali Safaeinili, Bruce A Campbell,  
995 Jeffrey J Plaut, Lucia Marinangeli, et al. Sharad sounding radar on the mars reconnaissance orbiter. *Journal of Geophysical Research:  
996 Planets*, 112(E5), 2007.
- 997 [77] Ph Paillou, G Grandjean, J-M Malézieux, G Ruffié, E Heggy, D Pignonier, P Dubois, and J Achache. Performances of ground penetrating  
998 radars in arid volcanic regions: Consequences for mars subsurface exploration. *Geophysical Research Letters*, 28(5):911–914, 2001.
- 999 [78] Federico Di Paolo, Sebastian E Lauro, Davide Castelletti, Giuseppe Mitri, Francesca Bovolo, Barbara Cosciotti, Elisabetta Mattei, Roberto  
1000 Orosei, Claudia Notarnicola, Lorenzo Bruzzone, et al. Radar signal penetration and horizons detection on europa through numerical  
1001 simulations. *IEEE Journal of Selected Topics in Applied Earth Observations and Remote Sensing*, 10(1):118–129, 2016.
- 1002 [79] Stefano Mottola, Gabriele Arnold, Hans-Georg Grothues, Ralf Jaumann, Harald Michaelis, Gerhard Neukum, and Jean-Pierre Bibring. The  
1003 rolis experiment on the rosetta lander. *Space Science Reviews*, 128:241–255, 02 2007. doi: 10.1007/s11214-006-9004-2.
- 1004 [80] Justin Maki, M. Golombek, Robert Deen, H. Abarca, C. Sorice, T. Goodsall, M. Schwochert, Mark Lemmon, Ashitey Trebi-ollennu, and  
1005 W. Banerdt. The color cameras on the insight lander. *Space Science Reviews*, 214, 09 2018. doi: 10.1007/s11214-018-0536-z.
- 1006 [81] P. Cambianica, G. Cremonese, G. Naletto, A. Lucchetti, M. Pajola, L. Penasa, E. Simioni, M. Massironi, S. Ferrari, D. Bodewits, F. La  
1007 Forgia, H. Sierks, P. L. Lamy, R. Rodrigo, D. Koschny, B. Davidsson, M. A. Barucci, J. L. Bertaux, I. Bertini, V. Da Deppo, S. Debei,  
1008 M. De Cecco, J. Deller, S. Fornasier, M. Fulle, P. J. Gutiérrez, C. Güttler, W. H. Ip, H. U. Keller, L. M. Lara, M. Lazzarin, Z. Y. Lin, J. J.  
1009 López-Moreno, F. Marzari, S. Mottola, X. Shi, F. Scholten, I. Toth, C. Tubiana, and J. B. Vincent. Quantitative analysis of isolated boulder  
1010 fields on comet 67P/Churyumov-Gerasimenko. *Astronomy & Astrophysics*, 630:A15, Oct 2019. doi: 10.1051/0004-6361/201834775.
- 1011 [82] I. Wright, S. Barber, Geraint Morgan, Andrew Morse, S. Sheridan, D. Andrews, J. Maynard, D. Yau, S. Evans, Mark Leese, John Zarnecki,  
1012 B. Kent, Nick Waltham, Martin Whalley, S Heys, D. Drummond, R. Edeson, E. Sawyer, R. Turner, and C. Pillinger. Ptolemy – an  
1013 instrument to measure stable isotopic ratios of key volatiles on a cometary nucleus. *Space Science Reviews*, 128:363–381, 02 2007. doi:  
1014 10.1007/s11214-006-9001-5.
- 1015 [83] J Grygorczuk, K Seweryn, R Przybyła, M Dobrowolski, B Kędziora, T Rybus, K Skocki, M Tokarz, R Wawrzaszek, et al. Priorities of the  
1016 smrl src pas involvement in exploration of the planetary bodies’ surface based on the existing and planned to be developed technologies. In  
1017 *2012 19th International Conference on Microwaves, Radar & Wireless Communications*, volume 2, pages 422–425. IEEE, 2012.
- 1018 [84] Karol Seweryn, J Grygorczuk, R Wawrzaszek, M Banaszkiwicz, T Rybus, et al. Low velocity penetrators (lvp) driven by hammering  
1019 action—definition of the principle of operation based on numerical models and experimental tests. *Acta Astronautica*, 99:303–317, 2014.
- 1020 [85] J Grygorczuk, Marek Banaszkiwicz, A Cichocki, Monika Ciesielska, M Dobrowolski, Bartosz Kędziora, J Krasowski, T Kuciński, M Mar-  
1021 czewski, Marek Morawski, et al. Advanced penetrators and hammering sampling devices for planetary body exploration. In *Proceedings of  
1022 the 11th symposium on advanced space technologies in robotics and automation, ESA/ESTEC, Noordwijk*, 2011.
- 1023 [86] A Trebi-Ollennu, Won Kim, Khaled Ali, Omair Khan, Cristina Sorice, Philip Bailey, Jeffrey Umland, Robert Bonitz, Constance Ciarleglio,  
1024 Jennifer Knight, et al. Insight mars lander robotics instrument deployment system. *Space Science Reviews*, 214(5):93, 2018.
- 1025 [87] OE Kozlov and TO Kozlova. Manipulators of the phobos-grunt project and lunar projects. In *Aerospace Robotics II*, pages 163–174.  
1026 Springer, 2015.
- 1027 [88] Mark Hutchins, Huw Simpson, and J Palencia Jiménez. Qinetiq’s t6 and t5 ion thruster electric propulsion system architectures and per-  
1028 formances. In *Joint Conference of 30th International Symposium on Space Technology and Science, 34th International Electric Propulsion  
1029 Conference, and 6th Nano-satellite Symposium*, 2015.
- 1030 [89] D. Murphy, M. Eskenazi, M. McEachen, and J. Spink. Ultraflex and megaflex - development of highly scalable solar power. *2015 IEEE  
1031 42nd Photovoltaic Specialist Conference (PVSC)*, pages 1–5, 06 2015. doi: 10.1109/PVSC.2015.7355945.
- 1032 [90] Rao Surampudi, Julian Blois, Ratnakumar Bugga, Erik Brandon, Marshall Smart, John Elliott, Julie Castillo, Thomas Yi, Leonine Lee,

- 1033 Mike Piszczor, Thomas Miller, Concha Reid, Chuck Taylor, Simon Liu, Ed Plichta, Christopher Iannello, Patricia M. Beauchamp, and  
 1034 James A. Cutts. Energy storage technologies for future planetary science missions. Technical report, NASA/Jet Propulsion Laboratory-  
 1035 Caltech, 2017.
- 1036 [91] Tatsuaki Hashimoto, Takashi Kubota, Jun'ichiro Kawaguchi, Masashi Uo, Kenichi Shirakawa, Takashi Kominato, and Hideo Morita. Vision-  
 1037 based guidance, navigation, and control of hayabusa spacecraft-lessons learned from real operation. *IFAC Proceedings Volumes*, 43(15):  
 1038 259–264, 2010.
- 1039 [92] Valerie C Thomas, Joseph M Makowski, G Mark Brown, John F McCarthy, Dominick Bruno, J Christopher Cardoso, W Michael Chiville,  
 1040 Thomas F Meyer, Kenneth E Nelson, Betina E Pavri, et al. The dawn spacecraft. In *The Dawn Mission to Minor Planets 4 Vesta and 1*  
 1041 *Ceres*, pages 175–249. Springer, 2011.
- 1042 [93] Yuichi Tsuda, Makoto Yoshikawa, Takanao Saiki, Satoru Nakazawa, and Sei-ichiro Watanabe. Hayabusa2–sample return and kinetic impact  
 1043 mission to near-earth asteroid ryugu. *Acta Astronautica*, 2018.
- 1044 [94] Ulrich Herfort and C Casas. Trajectory preparation for the approach of spacecraft rosetta to comet 67p/churyumov-gerasimenko. In  
 1045 *Proceedings 25 th International Symposium on Space Flight Dynamics-25 th ISSFD, Munich, Germany*, 2015.
- 1046 [95] B Williams, P Antreasian, E Carranza, C Jackman, J Leonard, D Nelson, B Page, D Stanbridge, D Wibben, K Williams, et al. Osiris-rex  
 1047 flight dynamics and navigation design. *Space Science Reviews*, 214(4):69, 2018.
- 1048 [96] Takahide Mizuno. Laser rangefinders for planetary exploration. In *Microoptics Conference (MOC), 2017 22nd*, pages 28–29. IEEE, 2017.
- 1049 [97] Chengchao Bai, Jifeng Guo, and Hongxing Zheng. Optimal guidance for planetary landing in hazardous terrains. *IEEE Transactions on*  
 1050 *Aerospace and Electronic Systems*, 2019.
- 1051 [98] Keyvan Kanani, Roland Brochard, Florent Hennart, Alexandre Pollini, Peter Sturm, Olivier Dubois-Matra, and Sanjay Vijendran. Sensor  
 1052 data fusion for hazard mapping and piloting. In *13th International Planetary Probe Workshop*, 2016.
- 1053 [99] K. Kanani, C. Robin, A. Masson, R. Brochard, P. Duteis, and R. Delage. Dual technologies to mature vision based navigation: the example  
 1054 of space rendezvous and air-to-air refueling. In *Proceedings of the 10th International ESA conference on Guidance, Navigation and Control*  
 1055 *Systems, Salzburg, Austria*, 2017.
- 1056 [100] Antoine Petit, Eric Marchand, and Keyvan Kanani. Tracking complex targets for space rendezvous and debris removal applications. In *2012*  
 1057 *IEEE/RSJ International Conference on Intelligent Robots and Systems*, pages 4483–4488. IEEE, 2012.
- 1058 [101] A Masson, C Haskamp, I Ahrns, R Brochard, P Duteis, K Kanani, and R Delage. Airbus ds vision based navigation solutions tested on liris  
 1059 experiment data. In *ESA 7th Space Debris Conference*, volume 2017, 2017.
- 1060 [102] Go Ono, Hitoshi Ikeda, Naoko Ogawa, Shota Kikushi, Fuyuto Terui, Takanao Saiki, and Yuichi Tsuda. Strategies and flight results of gnc  
 1061 system in hayabusa2 touchdown operations: Artificial landmark “target marker” separation and acquisition. In *AAS Guidance and Control*  
 1062 *Conference, Breckenridge, Colorado*, 2020.
- 1063 [103] Tetsuya Yamada, Toshio Ogasawara, Koichi Kitazono, and Hideyuki Tanno. High-speed compact entry capsule enhanced by lightweight  
 1064 ablator and crushable structure. *Transactions of the Japan Society for Aeronautical and Space Sciences, Aerospace Technology Japan*, 14  
 1065 (ists30):Pe\_33–Pe\_40, 2016.
- 1066 [104] Robert Dillman and James Corliss. Overview of the mars sample return earth entry vehicle. 2008.
- 1067 [105] Planetary Society. Cost of osiris-rex, 2020. URL <https://www.planetary.org/space-policy/cost-of-osiris-rex>.